Available online at www.sciencedirect.com

ScienceDirect

journal homepage: www.elsevier.com/locate/he

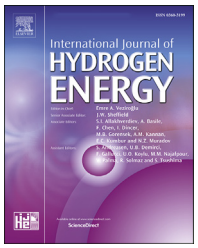

Techno-economic assessment of green hydrogen and ammonia production from wind and solar energy in Iran

Ali Kakavand [a], Saeed Sayadi [a,*], George Tsatsaronis [a], Ali Behbahaninia [b]

[a] Technische Universität Berlin, Chair of Energy Engineering and Environmental Protection, Marchstr. 18, D-10587 Berlin, Germany

[b] Department of Energy Systems Engineering, Faculty of Mechanical Engineering, K. N. Toosi University of Technology, Tehran, Iran

HIGHLIGHTS

- The minimum cost of green H2 in Iran was calculated to be between 2.94 and 3.32 USD/kgH_2.
- The minimum cost of green NH3 in Iran was obtained between 580 and 641 USD/tNH_3.
- H2 transportation via pipelines to the export harbor is the costliest scenario.
- More than two-thirds of the cost of NH3 is caused by the power generation system.
- Integrating green electricity into the Iranian grid is better than the P2A route.

ARTICLE INFO

Article history:
Received 27 October 2022
Received in revised form
15 December 2022
Accepted 24 December 2022
Available online 12 January 2023

Keywords:
Solar energy
Wind energy
Water electrolysis
Green ammonia
Green hydrogen
Seawater desalination

ABSTRACT

This paper presents a comprehensive technical and economic assessment of potential green hydrogen and ammonia production plants in different locations in Iran with strong wind and solar resources. The study was organized in five steps. First, regarding the wind density and solar PV potential data, three locations in Iran were chosen with the highest wind power, solar radiation, and a combination of both wind/solar energy. All these locations are inland spots, but since the produced ammonia is planned to be exported, it must be transported to the export harbor in the South of Iran. For comparison, a base case was also considered next to the export harbor with normal solar and wind potential, but no distance from the export harbor. In the second step, a similar large-scale hydrogen production facility with proton exchange membrane electrolyzers was modeled for all these locations using the HOMER Pro simulation platform. In the next step, the produced hydrogen and the nitrogen obtained from an air separation unit are supplied to a Haber-Bosch process to synthesize ammonia as a hydrogen carrier. Since water electrolysis requires a considerable amount of water with specific quality and because Iran suffers from water scarcity, this paper, unlike many similar research studies, addresses the challenges associated with the water supply system in the hydrogen production process. In this regard, in the fourth step of this study, it is assumed that seawater from the nearest sea is treated in a desalination plant and sent to the site locations. Finally, since this study intends to evaluate the possibility of green hydrogen export from Iran, a detailed piping model for the transportation of water, hydrogen, and ammonia from/to the production site and the export harbor is created in the last step, which considers the real routs using

* Corresponding author.
E-mail address: s.sayadi@tu-berlin.de (S. Sayadi).

https://doi.org/10.1016/j.ijhydene.2022.12.285

0360-3199/© 2022 Hydrogen Energy Publications LLC. Published by Elsevier Ltd. All rights reserved.

satellite images, and takes into account all pump/compression stations required to transport these media. This study provides a realistic cost of green hydrogen/ammonia production in Iran, which is ready to be exported, considering all related processes involved in the hydrogen supply chain.

© 2022 Hydrogen Energy Publications LLC. Published by Elsevier Ltd. All rights reserved.

Nomenclature

Roman Symbols

C	cost [USD]
$c_{p,mix}$	specific heat capacity at constant pressure for the mixture of nitrogen and hydrogen [kJ/kg ·K]
D	pipe outside diameter [m]
E	electricity [kW ·h]
f	Darcy friction factor [–]
F	modular factor for compressors, type factor for pumps [–]
F_d	design factor [–]
F_{sj}	seam joint factor [–]
F_t	transmission factor [–]
g	standard gravity = 9.81 [m/s^2]
H	pressure head [m]
i	real interest rate [–]
i′	nominal interest rate [–]
L	length [m]
$\dot{m}$	mass flow rate [kg/s]
n	project lifetime [year]
N	number [–]
p	pressure [bar]
P	power rate [kW]
P′	specific power rate [kW ·h/kg]
Q	volumetric flow rate [m^3/h]
$\dot{Q}$	heat transfer rate [kW]
r	inflation rate [–]
S	size factor [m$^{3.5}$/h]
SG	specific gravity [–]
S_h	hoop stress [?]
SV	salvage value [USD]
t	wall thickness of the pipes [m]
T	temperature [K]
v	velocity [m/s]

Greek Symbols

η	efficiency [–]
γ	specific heat ratio [–]
ρ	density [kg/m^3]

Subscripts

a	annualized
A	ammoniar
b	base
B	base (cost)
BM	bare module (cost)
C	compressor
CD	compressor drive
CS	compressor station
dis	discharge
d	design
DU	desalination unit
E	electricity
EL	electrolyzer
f	flow
H	hydrogen
HST	hydrogen storage tank
IC	intercooling
in	inlet
k	subscript for components
M	material
n	lifetime
out	outlet
P	pump
PS	pump station
r	replacement
s	isentropic
suc	suction
tot	total

Abbreviations

AST	Ammonia Storage Tank
ASU	Air Separation Unit
CAPEX	Capital Expenditure [USD]
CEPCI	Chemical Engineering Plant Cost Index
COP	Coefficient of Performance [–]
CRF	Capital Recovery Factor [–]
HHV	Higher Heating Value [kW ·h/kg]
IRENA	International Renewable Energy Agency
LCOA	Levelized Cost of Ammonia [USD/t_{NH_3}]
LCOE	Levelized Cost of Electricity USD/kW ·h
LCOH	Levelized Cost of Hydrogen [USD/kg_{H_2}]
MAFV	Maximum Allowable Fluid Velocity [m/s]
MAOP	Maximum Allowable Operating Pressure [bar]
MVC	Mechanical Vapor Compression
NIOC	National Iranian Oil Company
NPV	Net Present Value
NOX	Nitrogen Oxide
OPEX	Operational Expenditure [USD]
PEM	Proton Exchange Membrane
PV	Photovoltaic
SCADA	Supervisory Control and Data Acquisition
SMR	Steam Methane Reforming
SMYS	Specified Minimum Yield Strength [bar]
TDF	Temperature Derating Factor [–]

Introduction

Background

According to the Paris agreement in 2015, the net-zero carbon emission target must be reached by 2050, and the global temperature increase must be kept below 2 °C, preferably below 1.5 °C compared to the pre-industrial time [1]. This implies an extensive movement towards decarbonization in all sectors with contributions from all countries around the globe. As suggested by the International Renewable Energy Agency (IRENA), going in that direction entails cutting nearly 37 Gt CO_2 emissions annually by producing more electricity from renewable energy sources, increasing the efficiency of the energy conversion systems, vast electrification of end-use sectors, developing carbon capture and storage technologies, and producing green hydrogen and its derivatives [2].

Although renewable energy sources present record-breaking cost competitiveness, the intermittent nature of these energy resources reduces their reliability. To address this issue, batteries can be used for storing surplus energy. Batteries also have experienced a significant cost decline over the past decade [3] and they also enjoy a relatively high energy density. Nonetheless, the main shortcoming of batteries is the incapability of holding the energy for a long time [4]. Alternatively, the surplus electric energy can be transformed into chemicals and fuels for long-term electricity storage and for decarbonization purposes in sectors that are usually hard to decarbonize through electricity.

Hydrogen, in that perspective, can play a significant role in a zero-carbon emission future. It is an abundant element with a very high energy content per unit mass compared to many conventional fuels. Pressurized hydrogen contains approximately 40 kW•h/kg (based on the higher heating value), whereas the best Li-Ion batteries contain only around 0.28 kW•h/kg [5]. Hydrogen is also a robust alternative in Power-to-X technologies, with great potential for seasonal energy storage. Furthermore, the lack of carbon bonds makes it clean where it is combusted or goes through an electrochemical reaction in fuel cell systems [6].

Although hydrogen's energy content per unit mass is relatively high, its density at ambient temperature and pressure is extremely low, i.e., 0.083 kg/m^3. To store and cost-effectively transport hydrogen, it must be pressurized to 100–300 bar [7] or get it liquefied at temperatures below −250 °C. Either way is energy-intensive, which means the roundtrip efficiency of hydrogen conversion would be low. Therefore, it is recommended to use hydrogen to decarbonize industrial processes and not for electricity production [8].

Hydrogen can be produced from a variety of sources by using different technologies. Brown/black hydrogen is produced via a coal gasification process by converting the carbon-based compounds into the syngas consisting mainly of carbon monoxide and hydrogen. Coal gasification is considered the most environmentally damaging approach for hydrogen production. Currently, gray hydrogen, obtained from a Steam Methane Reforming (SMR) process, has the largest share among all types of hydrogen generation. Blue hydrogen production incorporates carbon capture and storage facilities to address the emission issues associated with gray hydrogen production. Similarly, turquoise hydrogen is produced through pyrolysis from the same feedstock as blue hydrogen [9]. Green and purple hydrogens are both obtained through an electrochemical reaction called electrolysis. The difference between them is the source of electricity production, which is renewable sources for green hydrogen, and nuclear energy for purple hydrogen.

Regarding direct environmental impacts, electrolysis is a clean technology. Nevertheless, depending on the type of electricity fed to the electrolyzer, there might be additional indirect impacts that must be considered. For instance, assuming 75% efficiency for a typical electrolyzer, if a conventional thermal power plant provides the required electricity, for 1 kg of the produced hydrogen, more than four tons of water must be withdrawn from rivers or seas for cooling systems in the power generation facility [10]. However, the direct required feed water for producing the same amount of hydrogen in an electrolysis process is only between 10 and 100 kg. Although, in some studies, this required direct water has been counted as the reason for the unsustainability of the electrolysis powered by renewables [11], it has been estimated that green hydrogen production requires 1.5 ppm of existing freshwater reserves or 30 ppb of saltwater in the world to cover the annual hydrogen demand [12]. These values are significantly lower than the water requirement for fossil fuel-based energy conversion facilities.

The cost of fossil-fuel-based hydrogen via SMR ranges from 0.8 to 2.7 USD/kg_{H_2} [13]. The given range depends mostly on the fossil fuel costs in the selected region. Usually, the lowest costs are obtained in the Middle East [14]. The current costs of green hydrogen are between 2.9 and 5.2 USD/kg_{H_2} [6,15,16]. Although the difference between the cost of green and fossil-based hydrogen is still remarkable, thanks to the continuous reductions in the cost of manufacturing electrolyzers and production of green electricity, and because of the recent energy crisis in Europe due to the Russian war against Ukraine, it is expected that the production of green hydrogen will become economically viable in the future.

As stated earlier, for hydrogen to be stored this needs to be either liquefied or compressed to high pressures, which are both energy-intensive. One solution to address these issues is converting hydrogen into another energy carrier, such as ammonia, which liquefies at −33 °C and ambient pressure or at 10 bar and room temperature [17], and does not react with stainless steel. Furthermore, the technology of producing ammonia is mature and well-established.

Ammonia is at the junction of energy and food, which makes it a crucial substance regarding population growth and climate change [18]. Ammonia can also be considered a clean fuel [19] without any carbon emissions. The same volume of ammonia contains around 50% more hydrogen than hydrogen does itself [20]. Unlike hydrogen, ammonia storage and transportation technologies are relatively inexpensive, simple, and mature [21]. Furthermore, the cost associated with ammonia storage is much lower than hydrogen and electricity storage [22]. Table 1 provides a comparison between ammonia and hydrogen.

Conventional ammonia production plants use an SMR process, which is energy intensive and is responsible for more

Table 1 – General comparison of compressed and liquid hydrogen with liquid ammonia [23].

Parameter	Compressed H_2	Liquid H_2	Liquid NH_3
Pressure [bar]	700	1	1
Temperature [°C]	–	−253	−33
Energy Density [kW•h/kg]	33.33	33.33	5.20
Energy Density [kW•h/L]	1.2	2.4	3.2
Required Energy for Storage	Medium	High	Low

than 2.5% of the global CO_2 emissions [18] and 1% of the global greenhouse gas emissions [17, 24]. This process needs to be decarbonized to reach the climate targets and eliminate the carbon footprint of the produced ammonia.

Currently, the specific cost of ammonia generated from fossil fuels is in the range of 220–550 USD/t_{NH_3} [17,25,26], which is significantly influenced by the coal and natural gas prices in the market. The cost of green ammonia strongly depends on the hydrogen production cost, which has been reduced over the last decade. Different studies reported different values for the specific cost of green ammonia, mainly because of financial assumptions, location, size of the plant, and interaction with the existing electricity grid. A cost range from 440 USD/t_{NH_3} in Saudi Arabia to more than 2000 USD/t_{NH_3} in other regions with poor renewable potentials has been reported in various studies [26–30].

Literature review

Realizing the net zero carbon emission future requires substantial exploitation of renewable sources, especially wind and solar energy. To reduce the mismatch between the demand and the intermittent supply, long-term sustainable energy storage is necessary [25]. The transformation of renewable energies into chemical materials such as hydrogen and ammonia offers the possibility for seasonal and large-scale storage. Moreover, green ammonia can significantly decarbonize the industries producing fertilizers [25].

Hong et al. [31] conducted a techno-economic analysis of hydrogen transportation, considering liquid hydrogen, liquid ammonia, compressed hydrogen, and methyl cyclohexane as hydrogen carriers. According to the findings of this study, using liquid hydrogen would result in the highest energy penalty. Moreover, it is concluded that the possibility of utilizing ammonia in the power industry makes it more advantageous compared to other hydrogen carriers.

Numerous studies assessed the feasibility of green hydrogen and ammonia production plants from the economic and environmental points of view. Arnaiz del Pozo et al. [26] performed an economic analysis for two low- and zero-carbon emission concepts for ammonia production: green electric-driven (without CO_2 emissions) and blue natural-gas-driven (with carbon capture and storage) ammonia production plants. These two concepts were compared with existing technologies, namely Kellogg-Braun and Root and Linde Ammonia Concept. According to this study, the specific cost of ammonia in the existing technologies is approximately 385 USD/t_{NH_3} in the European market, while the blue natural-gas-driven plant yields 332 USD/t_{NH_3}. Moreover, this study anticipates that the specific cost of green ammonia produced by hybrid wind and solar energies will be 772, 569, and 485 USD/t_{NH_3} in Germany, Spain, and Saudi Arabia in 2050.

Rivarolo et al. [23] investigated green ammonia production from hydroelectric power considering alkaline electrolyzers for hydrogen production. In this study, the specific cost of ammonia was obtained below 400 €/t_{NH_3} for production capacities between 200 and 1500 t_{NH_3}/d. The specific cost obtained from this study can compete with the market price for ammonia obtained from fossil-fuel-based production plants.

Rouwenhorst et al. [32] reviewed different hydrogen, nitrogen, and ammonia production and storage technologies in a decentralized energy system. This study also proposed a system consisting of available advanced technologies for ammonia production with a specific electricity consumption of 8.7–10.3 kW•h/kg_{NH_3}. Moreover, this study evaluates Ammonia-to-Power technologies such as solid oxide fuel cells. It was concluded that in northern Europe, a hybrid wind and solar off-grid system utilizing ammonia could be realized at a round-trip efficiency of 61%. The proposed system's final cost of electricity would be between 30 and 35 ¢/kW•h.

Ikäheimo et al. [24] evaluated power generation and district heating systems accompanied by long-term storage using the Power-to-Ammonia technology in Northern Europe. The power generation unit in this study is a hybrid system harnessing wind, hydro, and solar energies. The results indicated that the Power-to-Ammonia system would become an economically viable alternative if the natural gas price in Northern Europe goes above 70 €/MW•h or the carbon taxation passes 200 €/t_{CO_2}.

Pfromm [18] demonstrated that if electrically-driven hydrogen and nitrogen production units replace the conventional natural gas-based ones in industrial-scale ammonia plants, the energy demand would increase by 14%. This study indicated that since the largest share of energy demand comes from the hydrogen production sub-system, further improvements in Haber-Bosch catalysts would have a small impact on the energy footprint of the entire ammonia plant.

Maia [33] considered a scenario for 2030 with 12 GW of installed capacity for offshore wind turbines on an island in the North Sea. This study investigated eight configurations, including different locations for ammonia synthesis and various infrastructures for power transmission and ammonia and hydrogen transportation. Furthermore, alkaline and solid oxide electrolysis were considered for hydrogen production. Results of this study showed that the green ammonia produced in the best scenarios could compete with fossil-fuel-based ammonia only when it is accompanied by some incentives, such as green certificates.

Di Lullo et al. [34] compared the costs and the associated emissions of various hydrogen transportation systems. In this study, transporting pure hydrogen (via pipelines and trucks), hydrogen-natural gas blends (via pipelines), ammonia (via pipelines), and liquid organic hydrogen carrier (via pipelines and railways) were investigated. The results showed that transporting liquid carriers by trucks would cost more than hydrogen pipelines. Furthermore, the emission footprints of pure hydrogen and ammonia are almost half of the other carriers.

Armijo et al. [22] reported that the hybrid use of wind and solar energies could decrease the hydrogen and ammonia costs to below 2 USD/kg_{H_2} and 500 USD/t_{NH_3} in the near future.

Raab et al. [35] evaluated the combination of renewable energy sources and electricity from the grid to produce hydrogen in five locations around the world. According to this study, incorporating the grid assistance factor could reduce the final cost of hydrogen from 4 to 6 €/kg_{H_2} to around 2.5 €/kg_{H_2}.

Fasihi et al. [29] evaluated the global potential of renewable-based ammonia production from wind and solar sources. According to this comprehensive study, the best site throughout the world can produce green ammonia at a cost range of 440–630 USD/t_{NH_3}, 345–420 USD/t_{NH_3}, 300–330 USD/t_{NH_3}, and 260–290 USD/t_{NH_3} in 2020, 2030, 2040 and 2050, respectively. The findings of this study indicated that in 2030, green ammonia will be cost-competitive with the conventional one. However, applying the emission tax of 75 €/t_{CO_2} in 2040 will outweigh the fossil-fuel-based ammonia, regardless of the lowest possible natural gas price.

Smith et al. [36] showed that in an optimized electrically-driven ammonia synthesis, the rate of oxygen production from the electrolysis and air separation unit would be 1.4 kg_{O_2}/kg_{NH_3}. This oxygen can be sold to the medical sector, metallurgical industries, and power generation systems, bringing additional profit for electrically-driven ammonia production plants.

Bicer et al. [37] performed a life cycle assessment for different ammonia production routes. According to this study, electrically-driven ammonia production processes using nuclear energy had the lowest CO_2 emissions, equal to 0.48 kg_{CO_2}/kg_{NH_3}. This value for ammonia production using SMR and coal gasification is 1.9 and 2.55 kg_{CO_2}/kg_{NH_3}, respectively. If the system boundaries are chosen differently, and the complete supply chain for fossil fuels is taken into account, the CO_2 emissions for ammonia production via SMR and coal gasification would be 2.81 and 4.22 kg_{CO_2}/kg_{NH_3} [38].

A comparison between SMR and water electrolysis is shown in Ref. [39]. This study concluded that water scarcity and greenhouse gas emissions influence the selection of the best system differently. Ammonia production using the SMR process consumes less water but releases more emissions than electrically-driven ammonia production plants.

Erdemir and Dincer [40] studied the main challenges of using ammonia as a fuel, such as high ignition energy (8 MJ), low flame speed (0.15 m/s), and high NOX emissions. Fuel blending and exerting higher compression ratios are some proposed solutions in this study.

Contribution of the present study

This study presents a comprehensive technical design and economic assessment framework for a large-scale, electrically-driven green ammonia production plant. Furthermore, the impact of the location of harnessing renewable energy and the location of each sub-system on the final cost of the product has been examined. Unlike many similar studies, detailed design procedures and economic assessment for the power transmission and hydrogen and ammonia transportation sub-systems including pipelines and pressurization stations are considered in this study. Moreover, the complete supply chain for producing hydrogen, including the seawater desalination unit and the brine residual treatment system, is discussed in the present study.

Case study

Locations

The case study considered in this paper is Iran, with various renewable energy sources of high intensity and quality. The Caspian Sea and the Persian Gulf (gateway to international waters) surround Iran from the north and south. Water from these sources can directly supply the required water for the electrolysis process through pipelines. Moreover, the produced green ammonia can be exported to other countries through the southern and northern harbors.

In the central and southern parts of Iran, solar energy is accessible in very large amounts and with high durability [43]. According to the microscale wind data from the global wind atlas [41], the wind speed in the eastern regions of Iran is significantly high. In some locations, both solar and wind energies exist in great quantity and quality. Based on the annual meteorological data and other factors, such as accessibility (i.e., being close to the roads for transporting construction materials) and availability (i.e., not being too close to cities and residential areas) of the spot for constructing a plant, three locations are selected as potential sites, and one location is chosen as the base case for comparison purposes (see Fig. 1). In Neyriz, solar energy is more dominant than wind energy; in Sangan, wind energy is more powerful, and in Esfandak, wind and solar resources are both remarkable.

Scenarios

The impact of the selected locations on the technical and economic aspects of the green hydrogen/ammonia production plant is investigated through different scenarios. Since Iran suffers from water scarcity, and in most parts of the country, drought and very few rainfalls are being experienced [44–46], utilization of seawater for hydrogen production is more reasonable than water withdrawal from rivers, lakes, or underground resources. Therefore, in all selected locations, the nearest sea was chosen as the source of water supply for the electrolysis process.

In two scenarios, water is first desalinated near the sea and then transported to the selected locations shown in Fig. 1 because, due to the corrosivity of the seawater, its transportation would require corrosion-resistant materials for pipelines and would impose substantial capital and maintenance costs.

Unlike the desalination unit, the locations of power generation facilities and hydrogen and ammonia production plants differ in each scenario. Based on the location of the power generation, hydrogen production, and ammonia synthesis facilities, three scenarios are defined in this study and are depicted in Fig. 2.

Fig. 1 – Three inland locations with their closest distances from the export harbor and one base case at one of the export harbors in the South. Wind power density and specific daily PV power output for each spot are given on the map [41,42].

In the first scenario, only the power generation system is at the considered inland location, and all other facilities are placed next to the export harbor. The generated green electricity in the inland site is first fed to the national grid and then is taken from the grid at the export harbor considering the network losses in the Iranian national grid. This electricity provides the required power for the hydrogen and ammonia production plants and water desalination unit.

In the second scenario, except for the water desalination unit and ammonia storage tank, all other sub-systems are considered at the inland locations. In this case, desalinated water is transferred to the sites through underground water pipelines, and the produced liquid ammonia is transferred back to the export harbor via ammonia pipelines. Unlike the previous scenario, most of the generated electricity is consumed onsite, and only a small fraction is fed to the national grid to provide the required power for pressurization stations and the desalination unit.

In the third scenario, the hydrogen production facility and the power generation system are considered at the inland locations, and the rest are installed at the export harbor. The produced green hydrogen is transferred to the export harbor as compressed gas through pipelines and is fed to the Haber-Bosch process to produce ammonia near the sea.

In addition to these three scenarios, a reference plant is considered as the base case for comparison (Chabahar in Fig. 1), where all sub-systems are installed near the export harbor. In this case, the local wind and solar energy resources provide the required power for the entire ammonia production facility.

Plant design

This section explains the technical requirements and the design of all sub-systems of the proposed green ammonia production plant listed below.

- The power generation system from solar and wind resources consisting of wind turbines, photovoltaic panels, and batteries.
- Hydrogen and nitrogen production sub-systems including water desalination unit, PEM electrolyzers, air separation unit, and hydrogen storage tank.
- Ammonia synthesis and storage facilities.
- Transportation system including pipelines and all pressurization stations.

Fig. 3 depicts a process flow diagram of the entire plant. It must be noted that the water pump stations exist only in scenarios 2 and 3, the ammonia pump station only in scenario 2, and the hydrogen compressor stations only in scenario 3.

Electrolyzer

For this study, a Proton Exchange Membrane (PEM) electrolyzer was chosen because of its capability to operate in a wide

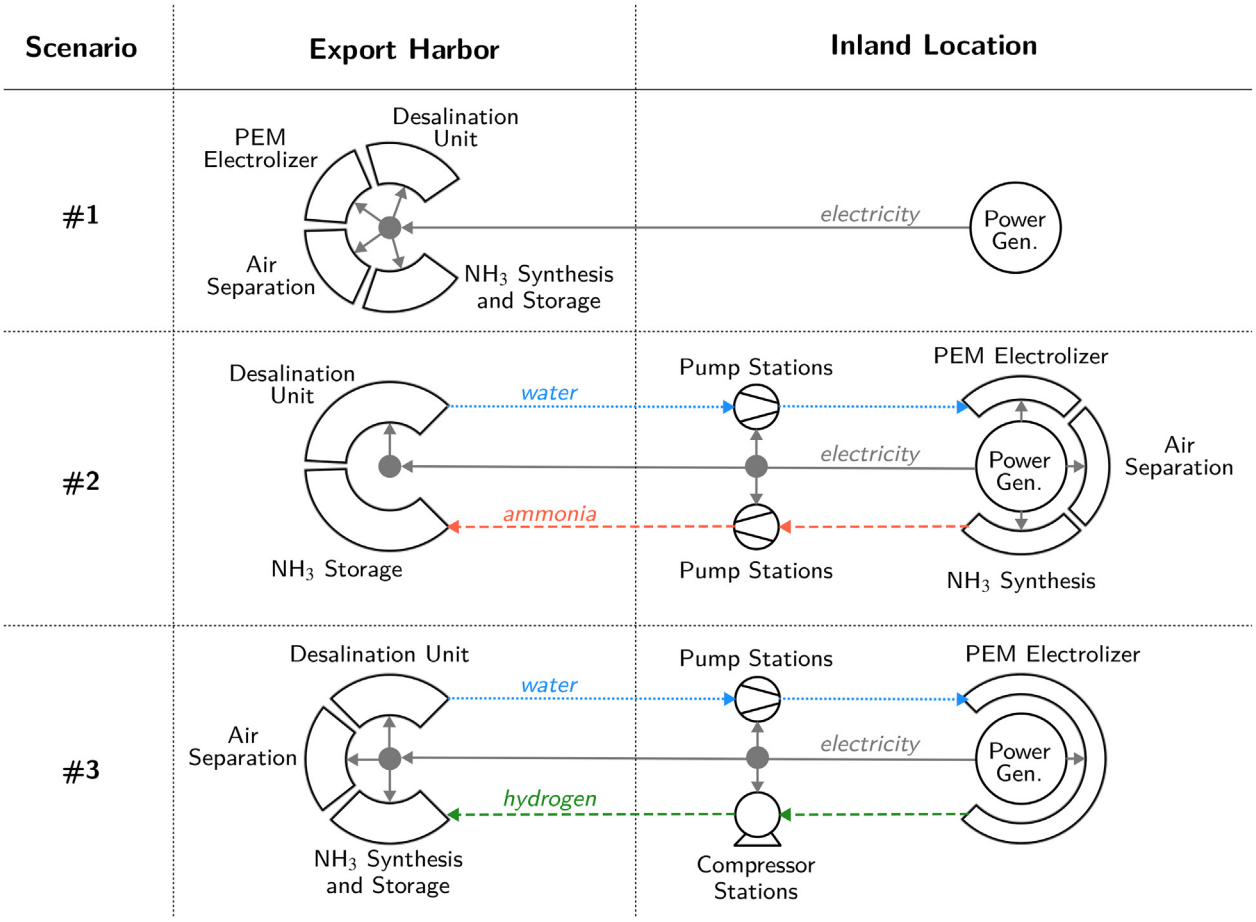

Fig. 2 – Three different scenarios for the layout of the green ammonia production plant. Dotted lines represent the water pipelines, dashed line represent the hydrogen and ammonia pipelines, and the solid lines show power transmission lines. (For interpretation of the references to color in this figure legend, the reader is referred to the Web version of this article.)

load range, quick response to demand variations, considerably low land footprint (>1 A/cm^2) [6,17,47], and higher operating pressure compared to alkaline anion exchange membranes. The technical data for this type of electrolyzer was taken from the NEL electrolyzers (model M5000) with a system efficiency of 70.9% [48].

Mass flow rates

All components of the proposed ammonia production plant, except electrolyzers, can be manufactured at large scales based on the existing technologies. In 2018, the manufacturing capacity of electrolyzers in the global market was approximately 135 MW [6], but currently, the manufacturing capacity of this component is 1 GW per year [6,48,49]. Since the hydrogen economy has attracted more attention in the past years, the manufacturers plan to scale up their capacities. For the present study, the installed capacity of the electrolyzers is considered 1 GW. Since the plant is hybrid and driven by wind and solar energies, a capacity factor of 50% is assumed. Based on these assumptions, the hydrogen mass flow rate in the proposed green ammonia production plant can be obtained from the following equation.

$$\dot{m}_{H_2}[kg/h] = \frac{installed\ capacity\ [kW] \times capacity\ factor[-] \times \eta_{EL}[-]}{HHV_{H_2}[kW \cdot h/kg]} \quad (1)$$

In Eq. (1), η_{EL} denotes the system efficiency of the considered electrolyzer given in the previous section. Based on the coefficients given in Table 2, the required mass flow rate of water, nitrogen, and ammonia are obtained once the mass flow rate of hydrogen is calculated.

Water desalination unit

In this study, the required water for the electrolysis process is provided from the seawaters in Iran. Although a built-in water purification equipment is installed on the electrolyzers, due to seawater's high amounts of salt and organic matter, an additional desalination unit is required to improve the electrolyzer's efficiency and lifetime [50].

In this paper, different desalination technologies have been studied, and finally, the Mechanical Vapor Compression (MVC) technology, which is electric-driven, was selected [50]. Compared to other water treatment technologies, MVC yields purer water, improving the stability and durability of the

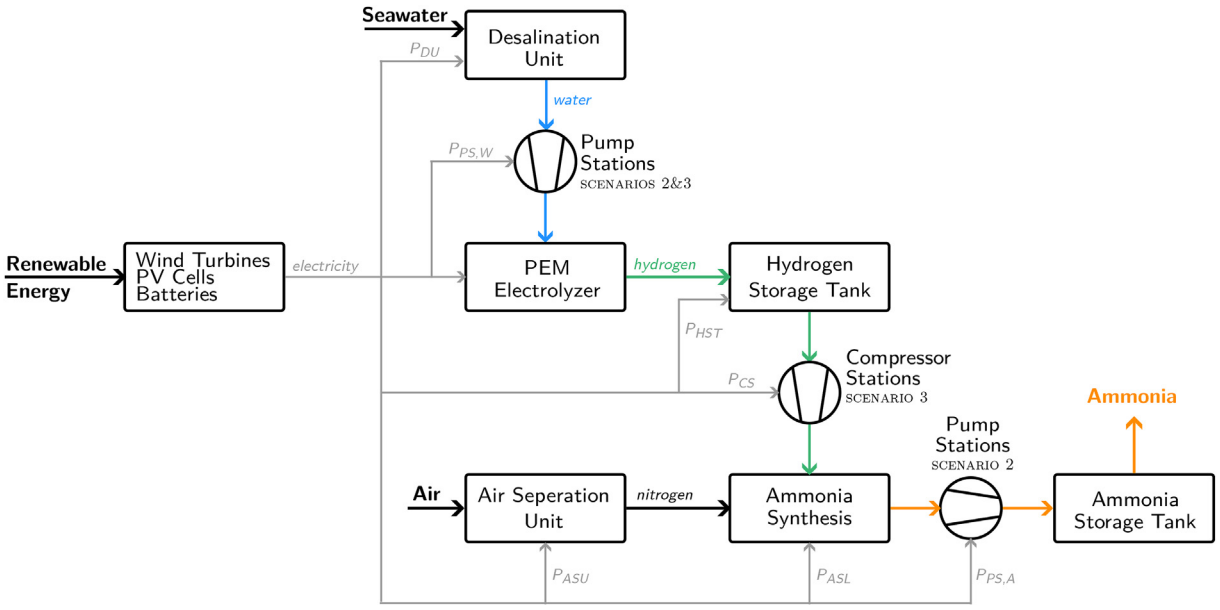

Fig. 3 – Process flow diagram of the proposed green ammonia production plant. (For interpretation of the references to color in this figure legend, the reader is referred to the Web version of this article.)

Table 2 – Mass flow rates of different mediums in an ammonia production plant.

Substance	Coefficient [kg/kg$_{H_2}$]	Mass flow rate [t/d]
Hydrogen	1.000	215.8
Desalinated Water	10.000	2157.9
Nitrogen	4.632	999.6
Ammonia	5.632	1215.3

considered PEM electrolyzer. Moreover, the possibility of heat integration with the PEM electrolyzer is another factor that makes the MVC more efficient. Nevertheless, this heat integration is only possible in the first scenario, where electrolyzers and the water desalination unit are installed in the same location. The provided capacity by this method is between 100 and 3000 t/d, which is in line with the requirement of the system being studied in this paper (see Table 2). The power consumption by the desalination unit is obtained from Eq. (2).

$$P_{DU} = \dot{m}_{H_2O} \cdot P'_{DU} \tag{2}$$

In the above equation, P'_{DU} is the specific power consumption of MVC technology, which is considered 22.8 kW·h/ t_{H_2O} [51].

One of the side effects of all desalination technologies is the brine residual. Leaving the generated brine untreated is unsustainable and environmentally harmful. The salt and other organic elements in the brine are useful in many applications and can be sold to the market as an additional product to bring some revenue to the project. In the present study, the "zero liquid discharge" technology has been considered for treating the brine produced from the seawater desalination unit [52].

Hydrogen storage tank

For large-scale applications, hydrogen can be stored in liquid and gas forms. The liquid hydrogen has a significantly higher energy density, but liquefaction is an energy-intensive process in which approximately 40% of the hydrogen's energy content are lost [53].

In the present study, hydrogen storage in gaseous form is considered, which is simpler and more efficient. It is assumed that hydrogen, after leaving the PEM electrolyzers at around 30 bar, gets pressurized up to 160 bar and stored in tanks. The storage tanks are assumed to be metal containers because of their low cost and simplicity of the technology. The power required for the mentioned compression process is calculated by Eq. (3), which is adapted from Refs. [54,55].

$$P_C = 97.5336 \times 10^{-6} \cdot \left(\frac{\gamma}{\gamma - 1}\right) \cdot Q \cdot T_{suc} \cdot N \cdot \left(\frac{Z_{suc} + Z_{dis}}{2}\right) \cdot \left(\frac{1}{\eta_{s,C}}\right) \cdot \left[\left[\left(\frac{p_{dis}}{p_{suc}}\right)^{\frac{1}{N}}\right]^{\frac{\gamma-1}{\gamma}} - 1\right] \tag{3}$$

Here, P_C [kW] is the required power for compression in the hydrogen storage tank, γ [–] is the specific heat ratio of hydrogen, Q [m^3/h] is the volumetric flow rate of hydrogen at standard conditions, T_{suc} [K] is the suction temperature, N is the number of compressor stages, p_{suc} and p_{dis} [bar] are the suction and discharge pressures of hydrogen, respectively, Z_{suc} and Z_{dis} [–] are the compressibility factors at suction and discharge conditions, respectively, and $\eta_{s,C}$ is the isentropic efficiency of the compressor, which is assumed to be 80%. In this study, all compressors are considered centrifugal because of their flexibility in handling large flow rates.

Furthermore, the hydrogen storage tank requires more power input for removing heat from several intercoolers between different compression stages. The needed electricity for compression in the hydrogen storage tank for the presented case study ($\dot{m}_{H_2} \approx 2.5$ kg/s) is 8638 kW. To remove the heat duty of the intercoolers (5532 kW) using a refrigeration machine with COP = 2.5, additional power of 2212 kW would be required. Therefore, the total power demand for the hydrogen storage tank is 10 850 kW.

The specific power consumption of the selected hydrogen storage tank can be obtained by dividing the total required power by the mass flow rates of the produced ammonia, as seen in Eq. (4). This specific parameter, similar to other specific power consumptions shown in this paper, is calculated based on the capacity of the plant, which makes it possible to compare power consumptions in different components of the system.

$$P'_{HST} = \frac{P_{HST}}{\dot{m}_{NH_3}} = 214.3 \text{ kW}\cdot\text{h} \Big/ \text{t}_{NH_3} \tag{4}$$

Air separation unit

The main objective of the air separation unit is to supply nitrogen to the ammonia synthesis loop. Oxygen is a valuable by-product of this process, which can be sold to the market and bring additional revenue to the project. In this paper, cryogenic distillation is considered for separating air because of its high nitrogen purity level, which is in the ppb (part per billion) range, and its large capacity, which can be up to 400 000 Nm3/h [29]. The power demand by the cryogenic distillation is mainly for the compressors used in the refrigeration cycle and is calculated from Eq. (5).

$$P_{ASU} = \dot{m}_{NH_3} \cdot P'_{ASU} \tag{5}$$

In the above equation, P_{ASU} [kW] is the power consumption of the considered air separation unit, $\dot{m}_{NH_3}$ [t/h] is the mass flow rate of the produced ammonia, and P'_{ASU} is the specific power consumption by the selected cryogenic air separation unit which is 90 $\text{kW}\cdot\text{h}/\text{t}_{NH_3}$.

Ammonia synthesis loop

A simplified schematic of the ammonia synthesis loop is presented in Fig. 4 [36]. Hydrogen and nitrogen are mixed outside the loop and are supplied as the feed to the synthesis loop. The feed gets pressurized to 200 bar after passing through the first compressor and mixed with the synthesis gas returning from the reactor. The mixture is supplied to the reactor after its temperature increases to 500 °C in a heat exchanger recovering the waste heat of the reactor. The synthesis gas is then fed to a fixed-bed catalytic reactor, which is the core of the synthesis loop. After this step, the produced ammonia is extracted using a condensation process, and the rest is recycled in the system. Because of the thermodynamics of the process, the rate of ammonia conversion in each cycle is only between 15% and 35% [36,56]. Therefore, the synthesis gas must repeat the process several times until it reaches the required purity level.

The required power for the synthesis loop is mainly for the compressor units, which is also obtained from Eq. (3). Since the difference between the inlet pressure of the feed stream and the loop's operating pressure is high, the compression process is done in several stages with intermediate coolers. The discharge temperature at each stage is calculated from Eq. (6), which is again reduced through intercoolers before entering the next compression stage.

$$T_{dis} = T_{suc} \cdot \left[\left(\frac{p_{dis}}{p_{suc}} \right)^{\frac{1}{N}} \right]^{\left(\frac{\gamma-1}{\gamma} \right)} \tag{6}$$

Once the outlet temperature of the compressor is calculated, the total heat transfer rate within intercoolers can be obtained using Eq. (7) [54].

$$\dot{Q}_{IC} = \dot{m} \cdot (N-1) \cdot \left(T_{IC,out} - T_{IC,in} \right) \cdot c_{p,mix} \tag{7}$$

In the above equations, $\dot{Q}_{IC}$ [kW] is the heat transfer rate, N is the number of compression stages, and $c_{p,mix}$ [kJ/kg·K] denotes the specific heat at a constant pressure for the mixture of nitrogen and hydrogen calculated from Ref. [57], and γ [–] is the specific heat ratio of the fluid.

For calculating the total power consumption of the synthesis loop, a conversion factor of 25% in each pass and five intermediate stages for compression units are considered. Moreover, the hydrogen pressure at the inlet of the synthesis loop is assumed to be 160 bar in scenarios 1, 2 and the base case, and 30 bar in scenario 3. Furthermore, in the synthesis loop, there is another compression unit with one intermediate stage for compensating the pressure drop within the loop, which is assumed to be 6% of the pressure in the synthesis loop [58]. The detailed design of the refrigeration machine to remove the heat from intercoolers is beyond the scope of this work, but to obtain its input power demand, a constant coefficient of performance (COP) of 2.5 is assumed. Finally, the specific power is found 309.6 $\text{kW}\cdot\text{h}/\text{t}_{NH_3}$ for scenarios 1, 2 and the base case, and 526.5 $\text{kW}\cdot\text{h}/\text{t}_{NH_3}$ for scenario 3, which is significantly higher than the specific power consumption of the hydrogen storage tank and air separation unit.

Ammonia storage tank

Ammonia is a toxic and flammable compound and can cause corrosion in tanks made of carbon steel materials; therefore, stainless steel tanks must be used for storing ammonia. It is assumed that ammonia is stored in liquid form at 10 bar and room temperature or at −33 °C and atmospheric pressure. The latter option was considered in the present paper, and a double-walled tank was selected to store liquid ammonia [59]. It was also assumed that the ammonia tank is designed for 30 days of storage.

Since some small portion of ammonia will be vaporized during the storage time, a refrigeration plant is considered to recover the vaporized ammonia. According to Ref. [60], the power consumption for a 9000-ton ammonia storage tank is approximately 17 kW. Similar to the hydrogen storage tank, this power demand is mainly needed for the compressors in the refrigeration plant. However, the power consumption of the ammonia storage tank was neglected in the current study because it is much lower than the power consumption in other processes of the considered hydrogen chain.

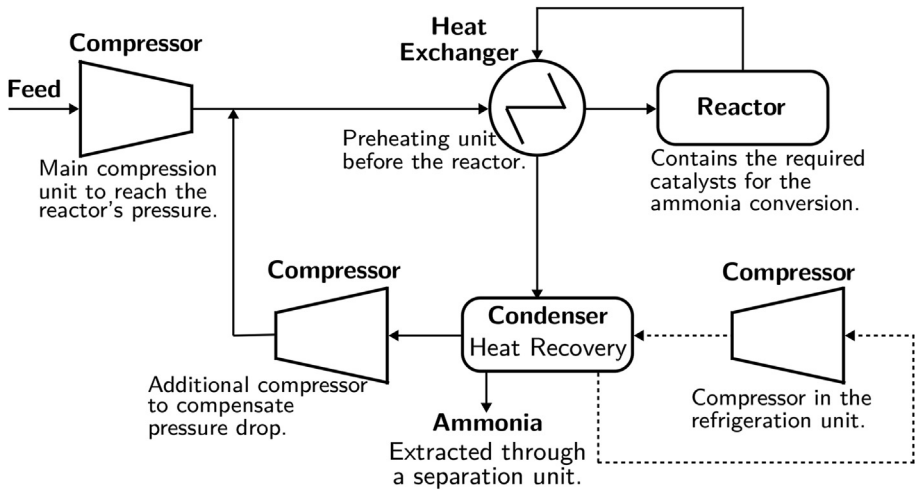

Fig. 4 – Simplified schematic of an ammonia synthesis loop adapted from Ref. [36].

Pipelines

The production capacity of the proposed plant is beyond the range of truck transportation, and therefore, pipeline transportation is considered in this study. One simple approach for designing the pipelines is to use some simplified correlations and rules of thumb to obtain pipe thicknesses and pumps and compressors' nominal capacities. Nevertheless, as the distance between sub-systems increases, inaccuracy in pipelines' calculations might lead to significant under- or overestimation of the project costs. For this reason, the present study proposes a detailed approach for obtaining the optimal characteristics of different pipelines and pressurization stations. Here, the pipelines are assumed to be straight, and their diameters and wall thicknesses remain the same along the piping route. Table 3 shows the main technical and design parameters for these pipelines.

The simplified flow model, seen in Eq. (8), was used for the initial estimation of the pipe diameter.

$$D = \sqrt{\frac{4 \cdot \dot{m}}{\pi \cdot \rho \cdot v}} \tag{8}$$

Here, $\dot{m}$ [kg/s] is the mass flow rate, ρ [kg/m^3] is the density of the fluid at flow temperature and average pressure along the pipeline, v [m/s] is the fluid velocity, and D [m] is the outside diameter of the pipe.

The hoop stress, S_h, is exerted along the circumference of the pipes and is a fraction of the Specified Minimum Yield Strength (SMYS) [63]. This fraction is called the *design factor* (F_d in Eq. (10)), which is usually considered 0.72 for non-residential areas [63]. However, for the initial calculation of the pipe's wall thickness, SMYS is considered as the maximum allowable value for the hoop stress. Based on the design pressures (p_d) in Table 3, and using Barlow's equation, Eq. (9), the initial wall thickness of the pipes can be calculated.

$$t = \frac{p_d \cdot D}{2S_h} \tag{9}$$

In the next step, the closest thickness in the ASME B36.10 M standard [67] to the calculated one is considered as the wall thickness. Then the flow velocity is calculated for this thickness; If it exceeds the MAFV in Table 3, either a smaller thickness according to the ASME B36.10 M standard or a larger pipe diameter will be selected.

All pipelines should withstand a given operating pressure, beyond which there would be a risk of pipeline failure. This pressure, known as the Maximum Allowable Operating Pressure (MAOP), is calculated from the modified Barlow's

Table 3 – Design parameters for the pipelines, which are all assumed underground.

	Compressed Hydrogen *Scenario 3*	Liquid Ammonia *Scenario 2*	Water *Scenarios 2 & 3*
Material [61, 62]	API 5L X42 PSL2	LTCS ASTM A333	CS ASTM A106 Gr.B
SMYS [bar]	2900	2400	2400
Design factor [–] [63]	0.72	0.72	0.72
MAFV [m/s] [64,65]	15	1.8	1.2
Design pressure [bar]	130	71	62
Roughness [mm] [66],	0.046	0.046	0.046

SMYS: Specified Minimum Yield Strength; MAFV: Maximum Allowable Fluid Velocity.

equation [66], Eq. (10), and will be used in the design of pressurization stations in the next section.

$$MAOP = \frac{2t \times SMYS \times F_{sj} \times F_d \times TDF}{D} \quad (10)$$

Here, $SMYS$ [bar] is the specified minimum yield strength, D [m] is the outside diameter, t [m] is the wall thickness, F_{sj} [–] is the seam joint factor, which is equal to 1 for seamless pipes, F_d [–] is the design factor, which is assumed to be 0.72 for this study, and TDF [–] is the temperature derating factor, which is 1 for temperatures below 121 °C (current study) and decreases to 0.867 when temperature increases to 230 °C.

The required pressure at the pipeline's origin must be calculated to deliver the fluid to the export harbor with a specific pressure. Eq. (11), which is adapted from Ref. [66], obtains this pressure for gas pipelines.

$$Q = 2.3944 \times 10^4 \times F_t \times \left(\frac{T_b}{p_b}\right) \times \left(\frac{p_1^2 - p_2^2}{SG \times T_f \times L \times Z}\right)^{0.5} \times D^{2.5} \quad (11)$$

In this equation, Q [m^3/h] is the volumetric flow rate, F_t [–] is the transmission factor, obtained by the Colebrook-White equation [68], T_b [K] and p_b [bar] are the base temperature and pressure considered for the pipeline design, p_1 and p_2 [bar] are the upstream and downstream pressures of the pipe segment, respectively, SG [–] is the specific gravity of the gas being transported, T_f [K] is the average flow temperature along the pipeline, L [m] is the length of the pipeline, Z is the compressibility factor of the fluid, and D [m] is the inside diameter of the pipeline.

For liquid pipelines, the pressure at the origin of the pipe consists of three major parts [69].

- The elevation head: this part depends on the variations in the terrain height along the pipe route.
- The delivery pressure: the required pressure at the delivery terminus in the export harbor.
- The frictional head: this parameter is calculated from the modified Darcy-Weisbach equation as shown in Eq. (12) [66].

$$\Delta p = f\left(\frac{L}{D}\right)\left(\frac{v^2}{2g}\right)\left(\frac{SG}{10.2}\right) \quad (12)$$

In the above equation, f [–] is the Darcy friction factor, L [m] is the pipe length, D [m] is the inner diameter of the pipe, v [m/s] is the average liquid velocity, g is the acceleration of gravity (9.81 m/s^2), and SG [–] is the specific gravity of the liquid.

Pressurization stations

Pump stations

The suction pressure for each pump, p_{suc}, should not drop below a specific range because operations at low suction pressures increase the probability of liquid vaporization resulting in cavitation [66]. In this study, it was assumed that the suction pressures of the pumps are 1.013 and 13.8 bar for water and ammonia pipelines, respectively. A pressure reduction below 10.3 bar would increase the risk of a phase change in ammonia. Considering the final discharge pressure at the origin, p_{dis}, and the maximum allowed operating pressure at stations (MAOP) obtained from Eq. (10), the number of required pump stations is calculated using Eq. (13). After rounding up the number of pump stations, the final discharge pressure is re-calculated using the same equation.

$$N_{PS} = (p_{dis} - p_{suc})/(MAOP - p_{suc}) \quad (13)$$

Eq. (14) calculates the brake hydraulic power of pump stations using the pressure head for each station obtained based on the suction and discharge pressures (H [m]), the volumetric flow rate of the fluid (Q [m^3/h]), the specific gravity (SG [–]), and the pump efficiency (η_P [–]), which is assumed 84% in this study. The power required by the electric drive to run the pump is obtained by dividing P_P by the electric drive efficiency, which is assumed to be 97%.

$$P_P = \frac{Q \cdot H \cdot SG}{367.46 \times \eta_P} \quad (14)$$

In the present study, one spare pump set is considered in each pump station to increase the reliability of the pressurization stations. Moreover, different pump capacities have been investigated, and, based on the results of the economic analysis, the most cost-effective one for each scenario was selected. For instance, in one case, two main pumps and one standby pump with capacities equal to 55% of the total capacity of the pump station are considered. In another case, three main pumps and one standby pump with capacities of 40% of the total capacity are selected.

Compressor stations

In a similar approach to the design of pump stations, MAOP is the indicator determining whether only one station at the origin suffices or more stations are needed along the pipe route. In some cases, the required inlet pressure of hydrogen to compensate for all pressure drops through the pipe route is less than the MAOP, which means only one compressor station at the beginning of the pipeline would be enough. In other cases, the required pressure at the origin of the pipeline becomes larger than the MAOP, which means intermediate compression stations along the pipeline route are needed.

The main challenge in designing compressor stations is to find the optimal number and location of the intermediate compression stations. It is possible that for the same operating condition and pipeline design, different numbers of compressor stations that can meet the requirements of the line are obtained. The more stations on the line, the smaller the stations and the lower the costs associated with each station would be. However, constructing more compression stations (even small ones) increases the total construction cost. Therefore, a trade-off exists to obtain the optimum number of stations along the pipeline.

After obtaining the number of stations, by using Eq. (11), the downstream pressure of each pipe segment can be calculated. This pressure corresponds to the suction pressure of the next station. The discharge pressure is equal to the MAOP calculated before. Knowing all the suction and discharge pressures of stations, the required power for each station is calculated using Eq. (3).

Like the pump stations, the power required by the electric drive to run the compressor is obtained through dividing the compressors' power consumption by the electric drive efficiency, which is assumed to be 95%.

Power transmission

The electricity needed for the pressurization stations and other system components explained in previous sections is provided by the hybrid wind-PV power generation facility designed for the proposed ammonia production plant. Since constructing a new power transmission network for this purpose is not economically viable, a better approach would be interacting with the Iranian national grid. In this way, the required power for the sub-systems and pressurization stations along the pipelines is purchased from the national grid. In return, the same amount of electricity is fed to the grid by the power generation plant. Moreover, depending on the scenario, the power generation facility provides all the electric losses in the Iranian grid for transporting the delivered electricity from the production site to the demand locations.

Economic analysis

General parameters

The nominal interest rate (i') in calculating the net present value of the project was considered 2.5% [70]. The real interest rate (i) is obtained using Eq. (15). In this equation, f denotes the expected inflation rate, which was assumed to be 1.5%.

$$i = \frac{i' - f}{1 + f} \tag{15}$$

At this point, the sum of all discounted values results in the net present cost of the project (C_{NPV}), which needs to be annualized using the Capital Recovery Factor (CRF) given in Eq. (16).

$$C_a = CRF(i,n)\cdot C_{NPV} = \frac{i(1+i)^n}{(1+i)^n - 1}\cdot C_{NPV} \tag{16}$$

In the above equation, n represents the project lifetime, which is considered to be 20 years.

Finally, the levelized cost of generated electricity, green hydrogen, and ammonia from wind and solar energy can be calculated using the following equations.

$$LCOE = \frac{C_{a,E}}{E_{tot}} \tag{17}$$

$$LCOH = \frac{C_{a,H}}{(\dot{m}_{H_2})_{tot}} \tag{18}$$

$$LCOA = \frac{C_{a,A}}{(\dot{m}_{NH_3})_{tot}} \tag{19}$$

In the above equation, $C_{a,E}$ [USD] refers to the annual cost of the components only in the power generation system (i.e., wind turbines, PV panels, batteries, and converters), and E_{tot} [kW•h] represents the total electricity produced in one year. For the calculation of LCOH [USD/kg_{H_2}], $C_{a,H}$ corresponds to the sum of the annual cost of the components in the hydrogen production sub-system (i.e., electrolyzers, hydrogen storage tank, and water desalination unit) and $C_{a,E}$. In the LCOA [USD/t_{NH_3}], the term $C_{a,A}$ denotes the total annual cost of the system.

Components costs

Table 4 summarizes specific CAPEX and OPEX, replacement cost, and lifetime for different components of the ammonia production plant. All costs given in this table are in 2021 USD and the assumptions made for obtaining them are explained in the following sections.

Electrolyzer

To obtain the cost of PEM electrolyzers used in this study, the International Renewable Energy Agency (IRENA) reports were considered. Many parameters affect the cost of electrolyzers. The module unit size and its potential for economy of scale, the manufacturing scale, and the advancement in technologies at cell levels are the most important ones. For this study, which is a large-scale hydrogen production plant, the module units of 25 MW (taken from the data sheet of the NEL electrolyzers, model M5000) and manufacturing scale of 1 GW per year were envisaged that results in the specific capital expenditure (CAPEX) of 600 USD/kW [6]. It can be seen in Ref. [6] that a decrease in the module size of the PEM

Table 4 – Specific capital and operational expenditures for all components of the green ammonia production plant.

Component	Specific CAPEX		Specific Annual OPEX		Lifetime [Years]
Power Generation					
Wind Turbine [3,70,71]	2000	USD/kW	44.0	USD/kW	25
PV System [3,70,72]	1164	USD/kW	9.3	USD/kW	30
Battery (Li-Ion) [73]	324	USD/kW•h	8.1	USD/kW•h	15
Hyrdogen Production					
Electrolyzer [6, 74, 75]	600	USD/kW[a]	18.1	USD/kW	25
Stack [6]	150	USD/kW	–		10
Storage Tank [76,77]	350	USD/kg_{H_2}	3.5	USD/kg_{H_2}	20
Water Desalination Unit [13,54,78,79]	531	USD/LPH	49.8	USD/LPH[b]	25
Nitrogen Production					
Air Separation Unit[c] [29, 80]	110	USD/t_{N_2}	1.6	USD/t_{N_2}	30
Ammonia Production					
Synthesis Loop[c] [24, 29, 54, 80]					
– Scenarios 1&2 and base case	569	USD/t_{NH_3}	8.5	USD/t_{NH_3}	30
– Scenario 3	712	USD/t_{NH_3}	10.7	USD/t_{NH_3}	30
Storage Tank [22, 29]	708	USD/t_{NH_3}	7.1	USD/t_{NH_3}	30

[a] Only for electrolyzers, the replacement cost is different from the CAPEX and is equal to 450 USD/kW.
[b] This value is obtained from 2.5% of the specific CAPEX plus 36.5 USD/LPH for brine treatment.
[c] All costs given for these components are relative to the annual amount of the produced nitrogen and ammonia.

electrolyzers increases the total cost of these components significantly. For instance, for PEM electrolyzer modules below 5 MW, the CAPEX would be between 1000 and 1300 USD/kW.

Material- and labor-related fixed operational expenditures (OPEX) are considered 1.5% and 1.52% of the specific CAPEX, respectively [74,75]. The variable OPEX is not considered here because the costs associated with electricity and water are already taken into account separately.

The lifetime of the electrolyzer units is assumed to be 25 years [74]. However, this value corresponds mainly to auxiliary components of the electrolyzer unit, such as heat exchangers, pumps, etc. The electrolyzer stack has a lifetime of 10 years [74,75,81] and needs to be replaces one time during the project lifetime (20 years). Therefore, only the auxiliary components are considered in the calculation of the salvage value of electrolyzers because there would be no more value in the stack after the 20th year of operation. The cost associated with the stack is assumed to be 25% of the electrolyzer's total capital cost [6].

Water desalination unit

Based on a study on the economic assessment of an MVC desalination unit producing 500 m^3 of desalinated water per day [54] and using the Chemical Engineering Plant Cost Index (CEPCI) for the years 2013 and 2021, the specific CAPEX for the water desalination unit designed for the presented system is estimated to be 531 USD/LPH.

As stated above, the brine treatment system is a complementary component of the water treatment system that reduces the environmental impacts of the proposed system by separating salts and other organic compounds. The discharge flow rate of the brine relative to the total inlet seawater is around 50% for the MVC technology [82]. According to Ref. [52], the cost of brine treatment using the zero liquid discharge system is 4.17 USD/m^3 of the flowing brine. This cost includes the capital required for the plant, crystallizer, and storage tanks, as well as the operating costs such as the required thermal and electric inputs.

Air separation unit

The CAPEX associated with the air separation unit is directly related to the mass flow rate of the produced nitrogen ($\dot{m}_{N_2}$) in [t/d] as seen in the following equation, which is adapted from Refs. [29,54].

$$CAPEX_{ASU} = 2.096 \times 10^6 \times \dot{m}_{N_2}^{-0.6249} + 12163 \quad (20)$$

The OPEX associated with the air separation unit is considered 1.5% of its CAPEX [80], and its lifetime is considered 30 years.

Ammonia synthesis loop and storage tank

The specific CAPEX for ammonia synthesis loop depends on the inlet hydrogen pressure which is different in the defined scenarios. It is considered 6239 USD/(kg(NH_3)/h) for scenario 3 because of its larger loop and 4983 USD/(kg(NH_3)/h) for scenarios 1, 2, and the base case [24,54]. The CAPEX [USD] of the ammonia storage tank is also given by Eq. (21), which is adapted from Ref. [29].

$$CAPEX_{AST} = 60.83 \times 10^3 \times m_{NH_3}^{-0.8636} + 700.8 \quad (21)$$

The lifetime of the stack in the catalytic reactor is 10 years and for the rest of the components in this sub-system it is 30 years [22,29]. The replacement cost of the stack is considered to be equal to 30% of the total CAPEX of the synthesis loop. Moreover, the OPEX of the ammonia synthesis loop and ammonia storage tank are 1.5% and 1% of their corresponding CAPEX, respectively [22,80].

Wind turbines

For the wind turbines, the economic data published by the International Renewable Energy Agency (IRENA) was considered [3]. Base on this data, the average CAPEX for onshore wind turbines in Asia (excluding China and India) is between 1334 and 3836 USD/kW (weighted average: 2472 USD/kW). Nevertheless, since Iran has taken many steps towards utilizing wind turbines in recent years, a CAPEX of 2000 USD/kW was considered for wind turbines in this study, which is lower than the weighted average cost.

Wind turbines are subjected to heavy and continuous loads, and therefore, it is assumed that the whole set needs to be replaced at the end of the lifetime, which is 25 years [3]. Another assumption is the overall loss factor of 4% for these components. According to Ref. [3], the specific OPEX for wind turbines vary between 33 and 56 USD/kW in different regions. In the present study, based on the recommendations in Ref. [70], 40 USD/kW is considered.

Solar PV system

A real project in Iran suggests specific CAPEX of 1791 USD/kW for the PV systems [72]. However, due to the global trend of cost reduction for PV systems from 2015 to 2021 [3], a 35% reduction in this cost in the Middle East region is assumed, resulting in 1164 USD/kW. According to Refs. [3,70], the specific OPEX of the selected PV systems is 9.3 USD/kW.

Although it is possible that after the end of the lifetime of the PV systems, the converters are still in good condition and do not need to be replaced, in this study, for simplicity, it was assumed that the entire PV system must be replaced.

Pressurization stations

For the cost estimation of the pressurization stations, Refs. [83,84] were used. Eq. (22) shows the general equation for calculating the bare module cost (C_{BM}) of the pumps and compressors.

$$C_{BM} = F \cdot F_M \cdot C_B \quad (22)$$

In the above equation, F is the modular factor for compressors and the type factor for pumps depending on the number of stages, case orientation, flow rate, and the shaft speed, F_M is the material factor, and C_B is the base cost of the considered equipment, which is also referred to as the purchased cost. C_B is estimated using the following equation for compressors and their electric drives, which is adapted from Ref. [83] and is valid for motor powers between 150 and 22 000 kW. P_{CD} was obtained by dividing P_C

from Eq. (3) by the motor efficiency of the compressors assumed to be 95%.

$$C_{B,CS} = \exp\{7.815 + 0.8 \times \ln(P_{CD})\} \quad (23)$$

The base costs for the pump and its electric drive are estimated separately. Eq. (24), which is adapted from Ref. [83], shows C_B for the pump considered in the present study, a single-stage centrifugal pump with a vertical split case made of cast iron operating at 3600 rpm.

$$C_{B,P} = \exp\left\{8.6911 - 0.3864[\ln(S)] + 0.0519[\ln(S)]^2\right\} \quad (24)$$

In the above equation, S denotes the size factor, which is a function of the volumetric flow rate of the liquid (Q [m^3/h]) and the pump head (H [m]) [83], as seen in the following equation.

$$S = Q\sqrt{H} \quad (25)$$

Unlike the compressor, the bare module cost for the electric drive of the pumps is separately estimated using Eq. (26), which is adapted from Ref. [83] and is valid for power in the range of 1–520 kW.

$$C_{BM,PD} = \exp\left\{5.8697 + 0.1697[\ln(P_{PD})] + 0.07662[\ln(P_{PD})]^2 + 0.024456[\ln(P_{PD})]^3 - 0.0035549[\ln(P_{PD})]^4\right\} \quad (26)$$

Here, P_{PD} is the required power by the electric drive which is calculated by dividing P_p from Eq. (14) by the motor efficiency, which is assumed to be 97%.

The total cost of the pressurization stations is not limited to rotary devices. Costs related to the fixed mechanical components and piping systems, electrical and wiring, instrument and control devices, safety, construction, and engineering costs should be considered too. Furthermore, according to the National Iranian Oil Company (NIOC), an additional cost associated with construction activities in regions of Iran far away from cities should also be considered [84]. The breakdown of all these costs for pumps and compressors is provided in Table 5.

Pipelines

Knowing the diameter and the wall thickness of the pipe, the weight of pipe segments per unit length is obtained using the ASME B36.10 M standard [67]. Then by multiplying the pipeline mass by the specific cost of steel, the pipeline material cost is obtained. Table 6 contains the specific costs per unit mass of different pipe materials.

After calculating the pipe material cost, according to Ref. [84], the piping installation costs and the costs associated with valves and fittings are estimated as 65% and 38% of the pipe material costs, respectively.

Finally, Table 7 shows the indirect costs of the transportation system, including pressurization stations and pipelines. This table shows that 67% of the costs are directly related to the pipelines and pressurization stations, estimated in the previous sections, while the remaining costs represent indirect costs.

Salvage value

Salvage value is the remained monetary value in equipment or facility when the project lifetime is reached. It is seen as revenue that occurs in the project's final year. Calculations regarding salvage values must be conducted for all components of the plant. For the kth component of the system, the salvage value is calculated using the following equation:

$$SV_k = C_{r,k} \times \left[(N_{r,k} + 1) - \frac{n}{n_k}\right] \quad (27)$$

Here, $N_{r,k}$ is the number of replacements of the component k during the project lifetime, n_k is the lifetime of the component k, n is the project lifetime, and $C_{r,k}$ [USD] is the replacement cost of the component being analyzed [85].

Table 5 – Breakdown of the total installed cost of pressurization stations constructed in Iran [84].

Cost Item			Compressors [%]	Pumps [%]
Equipment	Mechanical	Rortary	42	28
		Fixed	5	5
		Piping	8	10
	Electrical		3	13
	Instrument & Control		9	10
	Fire Fighting		5	5
Construction			22	22
Management and Engineering			6	7

Excess electricity

In 100% renewable energy systems, the optimal storage is usually not able to capture a considerable part of the excess energy, and therefore, some alternatives for utilizing this excess electricity should be considered. A common solution to deal with the excess electricity is converting it to heat and using it where needed or for lighting purposes in the plant area and near roads and cities. If there is no such usage for the excess electricity, it must be curtailed or dumped. In this study, selling the excess electricity to the main grid was also considered an option since there has been a gap between supply and demand in Iran's national grid in recent years.

For this reason and to encourage electricity production from renewable resources, the national grid management guarantees the purchase of green electricity for up to 10 MW production capacity. For plants with more than 10 MW capacities, Iran's Ministry of Energy must hold a tender. The feed-in tariff differs for renewable or non-renewable sources and peak or off-peak hours. Iran's inflation rate and political situation can also influence the feed-in tariffs. Nevertheless, in this study it was assumed that the feed-in rates are 500 Rls (0.02 USD) and 400 Rls (0.015 USD) per kW•h for peak and off-peak times, respectively, and a maximum of 4 h per day are considered as off-peak times [86].

Table 6 – Specific costs for various pipe materials.

Pipe Class	Fluid	Material Cost [USD/kg]
API 5L X42 PSL2	Hydrogen	2.8
LTCS ASTM A333 Gr.6	Ammonia	1.4
CS ASTM A106 Gr.B	Water	1.0

Table 7 – Indirect costs associated with pipelines in relation to the piping material and installation costs [84].

Item	Share [%]
Pipeline and Pressurization Stations	67
SCADA and Telecommunication System	3
Engineering and Construction Management	15
Right-of-Way Acquisition cost	5
Contingency	10
Total	100

Simulation

As described before, three inland locations with rich renewable sources in Iran were identified for harnessing renewable energies to power a green ammonia production plant. Three different scenarios (i.e., system layouts, see Fig. 2) were defined for each location resulting in 9 cases. Moreover, a base case scenario was considered for comparison purposes, in which all facilities, including the power generation system, were installed near the export harbor in the south of Iran.

The optimal capacities of the power generation and hydrogen production sub-systems, including PV panels, wind turbines, batteries, converters, electrolyzers, and the hydrogen storage tank, were obtained through simulations in the HOMER[1] Pro platform [85], which has been recently utilized as a modeling tool for simulating micro-grids in some studies [87,88]. The water desalination plant, air separation unit, and ammonia production facility were manually designed based on the HOMER Pro outputs.

Results and discussions

Levelized cost of the products

Levelized costs of electricity (LCOE), hydrogen (LCOH), and ammonia (LCOA) for different locations and scenarios are presented in Figs. 5–7. As seen in these figures, two costs are shown for each case. The less expensive one is calculated based on the assumption that the excess electricity produced by the power generation system due to the intermittency in renewable resources can be sold to the Iranian national grid. The more expensive value on these diagrams corresponds to the case that the excess electricity cannot be sold to the grid and must be dumped, which decreases the project's revenue and increases the final product costs.

Among all inland locations considered for power generation, in Neyriz, which mostly relies on solar energy, the products acquire the highest levelized costs, higher even when compared to the base case. Although in Neyriz, both solar and wind potentials are slightly greater than in the base case (see Fig. 1), the transportation system's impact on the final product cost leads to the higher costs. Nevertheless, the other locations in all scenarios resulted in less expensive products than the base case, implying that the impact of transportation costs on the final cost of the product can be offset by the quality of renewable resources.

According to Figs. 5–7, considering no electricity purchasing by the grid, the LCOE is between 2.7 and 5.2 ¢/kW•h, the LCOH is between 3.32 and 5.43 USD/kg_{H_2}, and the LCOA is between 641 and 1009 USD/t_{NH_3}. If the excess electricity can be sold to the national grid, products would become less expensive. In this case, the levelized cost for electricity would be in the range of 1.9 and 4.9 ¢/kW•h, for hydrogen between 2.94 and 5.16 USD/kg_{H_2}, and for ammonia from 580 to 960 USD/t_{NH_3}.

Figs. 5–7 also show that the third scenario for all locations produces the most expensive products. The reason is the costs associated with pressurizing and transporting hydrogen. Due to the physical properties of hydrogen, more expensive materials are required for the hydrogen pipeline than for other mediums. Furthermore, in scenario 3 the corresponding compression stage should reach the maximum pressure difference for hydrogen, namely from 30 bar to 200 bar.

Scenarios 1 and 2 yield very close levelized cost of electricity, hydrogen, and ammonia. In scenario 1, since all subsystems except the power generation are installed close to the export harbor, there is no cost of pipeline installation. However, since the generated power is sent to the other subsystems through the Iranian national grid, costs associated with power transmission losses are substantial. On the other hand, in scenario 2, transmission losses are minimal because only a small part of the generated power is sent to the pressurization stations, and the rest is used on-site for producing ammonia. So, these costs do not play a significant role. Instead, the costs of pipelines and pressurization stations for transporting water and ammonia are substantial.

In conclusion, the optimum layout for green hydrogen and ammonia production cannot be judged instantly. It must be thoroughly analyzed. Nevertheless, scenarios involving hydrogen transportation via pipelines are the costliest configurations and should be ruled out among other available alternatives.

As shown in Figs. 5–7, the produced electricity in Sangan is the least expensive among all other site locations. This spot has the highest potential for harnessing wind energy among all selected locations and can capture a very large yet highly intermittent amount of wind energy. For this reason, the share of excess electricity in this location is remarkably high. In Sangan, wind energy meets not only the demand of the entire plant but also goes beyond the capacity of batteries and hence, generates around 42% of excess electricity. If selling the excess electricity to the main grid is possible, Sangan will produce the least expensive products (LCOE = 1.9 ¢/kW •h, LCOH = 2.94 USD/kg_{H_2}, and LCOA = 580 USD/t_{NH_3}). But even if the excess electricity cannot be purchased by the Iranian national grid, the least expensive electricity will be still in Sangan (LCOE = 2.7 ¢/kW •h), whereas the other products will have the lowest costs in Esfandak (LCOH = 3.32 USD/kg_{H_2}, and 641 USD/t_{NH_3}). As seen in the diagrams, the amount of excess electricity in Esfandak is minimum (10.5% of the total generated electricity) which explains why the minimum and maximum costs given in Figs. 5–7 are closer compared to the other locations. In Esfandak, the impact of intermittency in renewable sources is significantly lower than in the other locations because of a well-balanced hybrid configuration of wind and solar energy, resulting in a smaller and better-sized layout for the plant which leads to lower product costs.

[1] Hybrid Optimization Model for Electric Renewables.

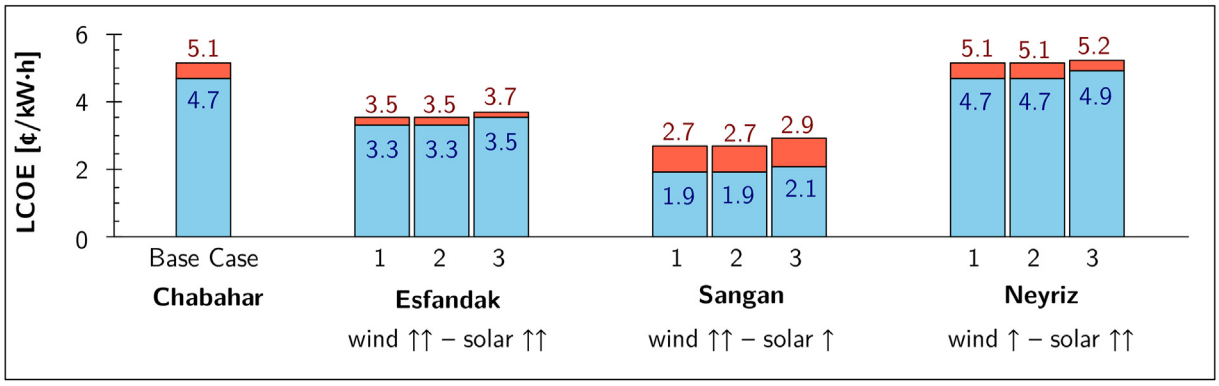

Fig. 5 – Levelized cost of electricity for all scenarios defined in this study for each location. The blue column corresponds to the case when the excess electricity can be sold to the Iranian national grid, and the red column shows the additional costs charged to the LCOE if the excess electricity cannot be sold to the grid. (For interpretation of the references to color in this figure legend, the reader is referred to the Web version of this article.)

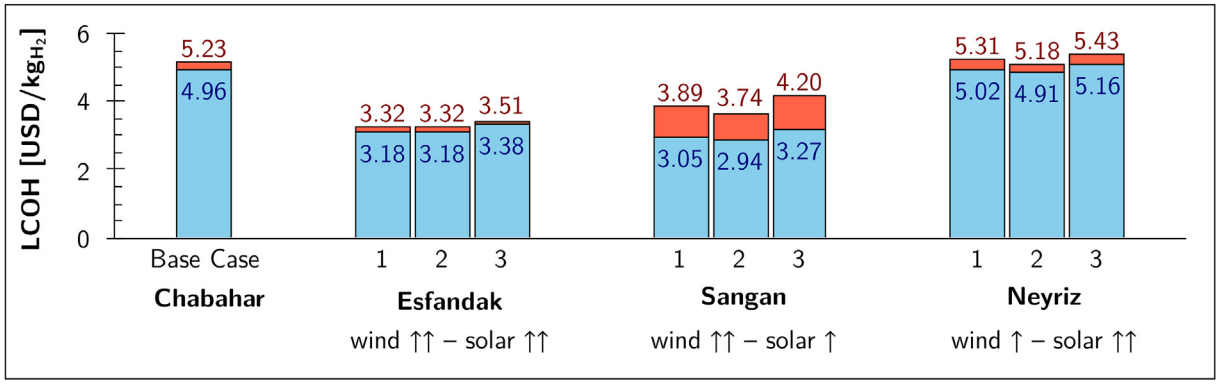

Fig. 6 – Levelized cost of hydrogen for all scenarios defined in this study for each location. The blue column corresponds to the case when the excess electricity can be sold to the Iranian national grid, and the red column shows the additional costs charged to the LCOH if the excess electricity cannot be sold to the grid. (For interpretation of the references to color in this figure legend, the reader is referred to the Web version of this article.)

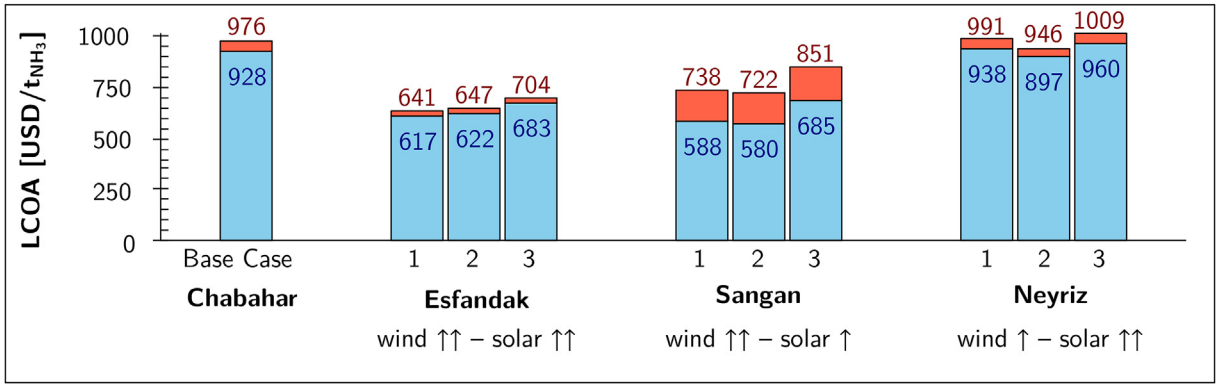

Fig. 7 – Levelized cost of ammonia for all scenarios defined in this study for each location. The blue column corresponds to the case when the excess electricity can be sold to the Iranian national grid, and the red column shows the additional costs charged to the LCOA if the excess electricity cannot be sold to the grid. (For interpretation of the references to color in this figure legend, the reader is referred to the Web version of this article.)

Table 8 – Contribution of each sub-system to the final cost of ammonia for the best scenario in each location.

Locations Sub-systems	Esfandak WIND ↑↑ – SOLAR ↑↑ *Scenario 1*	Sangan WIND ↑↑ – SOLAR ↑ *Scenario 2*	Neyriz WIND ↑ – SOLAR ↑↑ *Scenario 2*
Power Generation	**67.1%**	**66.5%**	**68.5%**
Wind Turbines	45.5%	58.0%	40.8%
PV System	15.6%	2.2%	22.1%
Batteries	5.8%	6.0%	5.4%
converters	0.3%	0.3%	0.2%
H_2 Production	**25.4%**	**21.4%**	**24.9%**
Electrolyzer	17.3%	15.0%	16.4%
Storage Tank	5.8%	4.4%	7.0%
Desalination Unit	2.3%	2.0%	1.5%
N_2 Production	**0.8%**	**0.7%**	**0.5%**
NH_3 Production	**6.7%**	**5.8%**	**4.4%**
Synthesis Loop	6.2%	5.4%	4.1%
Storage Tank	0.5%	0.4%	0.3%
Transportation	–	**5.6%**	**1.7%**
Pipelines	–	5.0%	1.4%
Pump Stations	–	0.6%	0.3%

Contribution of sub-systems to the final costs

Table 8 presents the contribution of each sub-system to the final cost of ammonia for the best scenario in each location. According to this table, the costliest sub-system is the power generation system, with a share of more than two-thirds of the final cost.

Power consumption of different components

Table 9 presents the excess electricity and power consumption of all components for the best scenario in each location. As shown in this table, most of the generated power is supplied to the water electrolysis in all cases, which is confirmed by the findings of other studies [18,32].

Moreover, it is shown that in Esfandak, thanks to the well-balanced hybrid configuration of wind and solar energy, the amount of excess electricity is minimal, resulting in lower product costs if this excess electricity cannot be sold to the grid. However, in Sangan, more than 40% of the produced electricity is not required by the plant and should either be dumped or sold to the national grid. The reason is that this location has a strong wind potential, which has higher intermittency than solar energy or hybrid wind/solar energy.

Table 9 also shows that the winner scenario for Esfandak is the first scenario, which considers only the power generation system in the inland location and all other facilities close to the export harbor. Therefore, unlike Sangan and Neyriz, pipelines and pressurization stations are not required for Esfandak.

For the transmission of the generated electricity in Esfandak to the export harbor, a loss of 6.7% per 1000 km of the transmission lines is assumed [89]. Therefore, to compensate for these losses, the amount of power required for electrolyzers is higher than in other cases.

Comparison of results with similar studies

The final cost of ammonia in all scenarios is calculated at an export harbor in the South of Iran to deliver to the global market. Indeed, the main focus of the present paper is on green ammonia production (and export) as a hydrogen carrier. As seen in Fig. 2, in the second scenario, which is the winning scenario in two locations (i.e., Sangan and Neyriz), hydrogen is produced and converted to ammonia in inland locations, but it is not sent to the export harbor. So, the LCOH values given in Fig. 6 represent the final cost of hydrogen in different locations in Iran. On the contrary, the LCOA values shown in Fig. 7, are all calculated at one location in Iran, the export harbor. For this reason, a comparison between the levelized cost of green ammonia in the present study with the average price in the market is very enlightening.

According to Ref. [90], the ammonia price in the North American market during the fourth quarter of 2021 reached 1177 USD/t_{NH_3}. In December 2021, the ammonia price in Germany reached 934 USD/t_{NH_3}. China experienced 702 USD/t_{NH_3} in the third quarter of 2021; in India, the prices were 798 USD/t_{NH_3}. However, in the first half of 2021, the ammonia prices in the USA were 330–450 USD/t_{NH_3}, respectively, whereas prices in India reached 362 USD/t_{NH_3} in the second quarter of the same year. These values show a considerable fluctuation in the ammonia market prices mainly because of

Table 9 – Power consumption of each component and its share related to the total power generation for the best scenario in each location.

Locations Components	Esfandak WIND ↑↑ – SOLAR ↑↑ *Scenario 1*		Sangan WIND ↑↑ – SOLAR ↑ *Scenario 2*		Neyriz WIND ↑ – SOLAR ↑↑ *Scenario 2*	
	[kW•h/t_{NH_3}]	[%]	[kW•h/t_{NH_3}]	[%]	[kW•h/t_{NH_3}]	[%]
Electrolyzer	10 296	84.2	9958	55.0	9983	75.6
Hydrogen Storage Tank	214	1.8	214	1.2	213	1.6
Desalination Unit	41	0.3	41	0.2	41	0.3
Air Separation Unit	90	0.7	90	0.5	90	0.7
Ammonia Synthesis Loop	310	2.5	310	1.7	309	2.3
Pressurization Stations	–	–	83	0.5	47	0.4
Excess Electricity	1276	10.5	7400	40.9	2528	19.1
Total Power Generation	**12 227**	100	**18 096**	100	**13 211**	100

the variation in the natural gas prices in different countries. All the market prices are associated with gray ammonia and depend on natural gas and coal prices.

Despite the relatively high capital cost of wind turbines and PV systems in Iran, the obtained cost for green ammonia in Iran compared to the current gray ammonia prices is very promising. It must be noted that the market prices are significantly affected by the natural gas price variations as a result of multiple crises such as the Russian war against Ukraine, the consequent energy-related conflicts in Europe, and the impact of COVID-19 on all economies in the world. In this situation, promoting green ammonia production in countries such as Iran with rich renewable resources can rise to the mentioned challenges and facilitate the decarbonization efforts around the world.

Furthermore, a comparison of the results of the present paper with another study investigating the potential locations for producing green ammonia at low cost is presented in Table 10. It shows that two locations in the current research belong to the top ten potential locations with low production costs.

Environmental impacts

Another aspect of this study is to evaluate the amount of avoided CO_2 emissions by producing ammonia using green electricity instead of other production methods from fossil fuels. According to Ref. [91], the CO_2 emission of a conventional ammonia plant is 1.694 CO_2/t_{NH_3}. As calculated before, the proposed ammonia plant can produce approximately 443 000 t_{NH_3} per year, saving more than 0.75 million tons of CO_2 annually.

It should be mentioned, however, that the reduction in the worldwide CO_2 emissions would be higher if the produced green electricity were initially used directly in the Iranian grid to reduce the fossil fuel usage for electricity generation in Iran [92]. Nevertheless, this, on the one hand, requires political courage and proper taxation/penalties on fossil fuel consumption. On the other hand, it makes the regulation and management of the national grid more complex after integrating more renewable energies with high uncertainty.

Table 10 – Potential green ammonia production plants with a predicted low production cost [27].

Country	Location	LCOA [USD/t_{NH_3}]
Australia	Cape Grim	473
Austria	Sonnblick	518
Denmark	List	528
Ireland	Malin Head	554
Russia	Dickson island	565
Iran (current study: with selling the excess electricity)	*Sangan*	580
UK	Lerwick	584
India	Jodhpur	636
Iran (current study: without selling the excess electricity)	*Esfandak*	641
Senegal	Dakar	661

In an *ideal* situation, if the integration of the generated green electricity into the Iranian national grid would be possible, it could reduce the worldwide CO_2 emission up to 2.8 times more than if it is used for green ammonia production and export to other countries [93]. This is because of the high CO_2 emissions from the power mix of Iran, which is, on average, 584.5 $t_{CO_2}/GW{\cdot}h$ of generated electricity. However, for countries with cleaner power grids, such as Denmark, with 155 $t_{CO_2}/GW{\cdot}h$ [94], the difference in CO_2 savings through hydrogen production and grid decarbonization is relatively small.

From the grid administration viewpoint, feeding green electricity to the national grid would be attractive only when the electricity is provided without or at least with minimum fluctuations. The highly intermittent nature of wind and solar energies would require a substantial number of batteries to reduce these fluctuations. This imposes a high cost and increases the environmental impacts because of the batteries use. This seems an interesting topic that can be addressed in a separate study. Nevertheless, in green hydrogen and ammonia production routes, the required number of batteries is significantly lower due to the use of hydrogen storage tanks to improve the balance between supply and demand. Therefore, in *real* situations, in the absence of the required infrastructure for integrating the green electricity into the grid, green hydrogen/ammonia production and export would be the second-best choice to benefit from the rich solar and wind resources in regions like Iran, which can contribute to the industrial decarbonization around the world, but not with the full potential of these resources (due to the inefficiencies involved in the hydrogen/ammonia production processes).

Conclusions

In the present study we performed a comprehensive technical and economic assessment of a green hydrogen/ammonia production plant in different locations with rich renewable potentials in Iran. The final cost of ammonia is calculated at an export harbor in the South of Iran, for ammonia to be delivered to the global market. According to the results of this study, the following conclusions can be drawn.

1. When the excess electricity can be sold to the Iranian national grid, the minimum levelized cost of green hydrogen and ammonia would be 2.94 USD/kg_{H_2} and 580 USD/t_{NH_3}, respectively. But if the generated excess electricity cannot be sold to the grid, the minimum costs would be 3.32 USD/kg_{H_2} and 641 USD/t_{NH_3}, respectively.
2. In many cases, with hundreds of kilometers of distance from the export harbor, the final products are less expensive than those of the base case, which is considered to operate at the export harbor. This indicates that the monetary savings through harnessing high-quality renewable resources in those locations outweigh the costs associated with transporting products from the selected locations to the export harbor.
3. Almost in all inland locations chosen in the present study, the costliest scenario was the one considering hydrogen

transportation through pipelines from the selected locations to the export harbor.

4. In all scenarios, more than two-thirds of the final cost of ammonia came from the power generation system, which had the highest contribution among all sub-systems. The total installed cost of wind and solar farms in Iran is relatively high. However, there has been a continuous reduction in these costs in the past decade, which means the levelized cost of green ammonia is expected to be lower in the future. For instance, a 25% reduction in the cost of wind turbines and PV systems would decrease the levelized cost of ammonia by 16%.
5. From an environmental (decarbonization) viewpoint, the Power-to-Ammonia route in Iran is the second-best choice compared to the direct integration of the generated green electricity into the Iranian national grid. Nevertheless, if the carbon intensity of the power mix in a country is low (e.g., in Denmark), moving towards Power-to-X routes would become more meaningful.

Declaration of competing interest

The authors declare that they have no known competing financial interests or personal relationships that could have appeared to influence the work reported in this paper.

REFERENCES

[1] Paris agreement. 2016. https://unfccc.int/process-and-meetings/the-paris-agreement/the-paris-agreement.

[2] IRENA. World energy transitions outlook 2022: 1.5°C pathway, Abu Dhabi. 2022. https://irena.org/publications/2022/mar/world-energy-transitions-outlook-2022.

[3] IRENA. Renewable power generation costs in 2020. Abu Dhabi 2021. https://www.irena.org/publications/2021/Jun/Renewable-Power-Costs-in-2020.

[4] Faria JA. Renaissance of ammonia synthesis for sustainable production of energy and fertilizers. Current Opinion in Green and Sustainable Chemistry 2021;29:100466. https://doi.org/10.1016/j.cogsc.2021.100466.

[5] Liu Y-T, Liu S, Li G-R, Gao X-P. Strategy of enhancing the volumetric energy density for lithium-sulfur batteries. Adv Mater 2021;33(8):e2003955. https://doi.org/10.1002/adma.202003955. Deerfield Beach, Fla.

[6] IRENA. Green hydrogen cost reduction: scaling up electrolysers to meet the 1.5°C climate goal. Abu Dhabi 2020. https://www.irena.org/publications/2020/Dec/Green-hydrogen-cost-reduction.

[7] Abdalla AM, Hossain S, Nisfindy OB, Azad AT, Dawood M, Azad AK. Hydrogen production, storage, transportation and key challenges with applications: a review,. Energy Convers Manag 2018;165:602–27. https://doi.org/10.1016/j.enconman.2018.03.088.

[8] Papadis E, Tsatsaronis G. Challenges in the decarbonization of the energy sector. Energy 2020;205:118025. https://doi.org/10.1016/j.energy.2020.118025.

[9] Laguna JC, Duerinck J, Meinke-Hubeny F, Valee J. Carbon-free steel production: cost reduction options and usage of existing gas infrastructure, European Parliament and Directorate-General for Parliamentary Research Services. 2021. https://doi.org/10.2861/01969.

[10] Webber ME. The water intensity of the transitional hydrogen economy. Environ Res Lett 2007;2(3):034007. https://doi.org/10.1088/1748-9326/2/3/034007.

[11] Bossel U. Does a hydrogen economy make sense?, Proceedings of the IEEEvol. 94; 2006. p. 1826–37. https://doi.org/10.1109/JPROC.2006.883715. 10.

[12] Beswick RR, Oliveira AM, Yan Y. Does the green hydrogen economy have a water problem? ACS Energy Lett 2021;6(9):3167–9. https://doi.org/10.1021/acsenergylett.1c01375.

[13] Singlitico A, Østergaard J, Chatzivasileiadis S. Onshore, offshore or in-turbine electrolysis? techno-economic overview of alternative integration designs for green hydrogen production into offshore wind power hubs. Renewable and Sustainable Energy Transition 2021;1:100005. https://doi.org/10.1016/j.rset.2021.100005.

[14] International Energy Agency (IEA). The future of hydrogen: seizing today's opportunities, Japan. 2019. https://www.iea.org/reports/the-future-of-hydrogen.

[15] Yates J, Daiyan R, Patterson R, Egan R, Amal R, Ho-Baille A, Chang NL. Techno-economic analysis of hydrogen electrolysis from off-grid stand-alone photovoltaics incorporating uncertainty analysis. Cell Reports Physical Science 2020;1(10):100209. https://doi.org/10.1016/j.xcrp.2020.100209.

[16] Bruce S, Temminghoff M, Hayward J, Schmidt E, Munnings C, Palfreyman D, Hartley P. National hydrogen roadmap: pathways to an economically sustainable hydrogen industry in Australia. Aust Now 2018. https://www.climatecollege.unimelb.edu.au/seminar/pathways-economically-sustainable-hydrogen-industry-australia.

[17] MacFarlane DR, Cherepanov PV, Choi J, Suryanto BH, Hodgetts RY, Bakker JM, Ferrero Vallana FM, Simonov AN. A roadmap to the ammonia economy. Joule 2020;4(6):1186–205. https://doi.org/10.1016/j.joule.2020.04.004.

[18] Pfromm PH. Towards sustainable agriculture: fossil-free ammonia. J Renew Sustain Energy 2017;9(3):034702. https://doi.org/10.1063/1.4985090.

[19] Lan R, Irvine JT, Tao S. Ammonia and related chemicals as potential indirect hydrogen storage materials. Int J Hydrogen Energy 2012;37(2):1482–94. https://doi.org/10.1016/j.ijhydene.2011.10.004.

[20] Thomas G, Parks G. Potential roles of ammonia in a hydrogen economy. 2006. https://www.energy.gov/sites/prod/files/2015/01/f19/fcto_nh3_h2_storage_white_paper_2006.pdf.

[21] Makepeace JW, He T, Weidenthaler C, Jensen TR, Chang F, Vegge T, Ngene P, Kojima Y, de Jongh PE, Chen P, David WI. Reversible ammonia-based and liquid organic hydrogen carriers for high-density hydrogen storage: recent progress. Int J Hydrogen Energy 2019;44(15):7746–67. https://doi.org/10.1016/j.ijhydene.2019.01.144.

[22] Armijo J, Philibert C. Flexible production of green hydrogen and ammonia from variable solar and wind energy: case study of Chile and Argentina. Int J Hydrogen Energy 2020;45(3):1541–58. https://doi.org/10.1016/j.ijhydene.2019.11.028.

[23] Rivarolo M, Riveros-Godoy G, Magistri L, Massardo AF. Clean hydrogen and ammonia synthesis in Paraguay from the itaipu 14 gw hydroelectric plant. ChemEngineering 2019;3(4):87. https://doi.org/10.3390/chemengineering3040087.

[24] Ikäheimo J, Kiviluoma J, Weiss R, Holttinen H. Power-to-ammonia in future north european 100 % renewable power and heat system. Int J Hydrogen Energy

2018;43(36):17295–308. https://doi.org/10.1016/j.ijhydene.2018.06.121.
[25] Ammonia: zero-carbon fertiliser, fuel and energy store, London. 2020. https://royalsociety.org/topics-policy/projects/low-carbon-energy-programme/green-ammonia/.
[26] Del Arnaiz Pozo C, Cloete S. Techno-economic assessment of blue and green ammonia as energy carriers in a low-carbon future. Energy Convers Manag 2022;255:115312. https://doi.org/10.1016/j.enconman.2022.115312.
[27] Nayak-Luke R, Forbes C, Cesaro Z, Bañares-Alcántara R, Rouwenhorst K. Chapter 8-techno-economic aspects of production, storage and distribution of ammonia. In: Valera-Medina A, Banares-Alcantara R, editors. Techno-economic challenges of green ammonia as an energy Vector. Academic Press; 2021. p. 191–207. https://doi.org/10.1016/B978-0-12-820560-0.00008-4.
[28] Nosherwani SA, Neto RC. Techno-economic assessment of commercial ammonia synthesis methods in coastal areas of Germany. J Energy Storage 2021;34:102201. https://doi.org/10.1016/j.est.2020.102201.
[29] Fasihi M, Weiss R, Savolainen J, Breyer C. Global potential of green ammonia based on hybrid pv-wind power plants. Appl Energy 2021;294:116170. https://doi.org/10.1016/j.apenergy.2020.116170.
[30] Hydrogen insights: a perspective on hydrogen investment, market development and cost competitiveness. 2021. https://hydrogencouncil.com/wp-content/uploads/2021/02/Hydrogen-Insights-2021.pdf.
[31] Hong X, Thaore VB, Karimi IA, Farooq S, Wang X, Usadi AK, Chapman BR, Johnson RA. Techno-enviro-economic analyses of hydrogen supply chains with an asean case study. Int J Hydrogen Energy 2021;46(65):32914–28. https://doi.org/10.1016/j.ijhydene.2021.07.138. https://www.sciencedirect.com/science/article/pii/S0360319921028329.
[32] Rouwenhorst KH, van der Ham AG, Mul G, Kersten SR. Islanded ammonia power systems: technology review & conceptual process design. Renew Sustain Energy Rev 2019;114:109339. https://doi.org/10.1016/j.rser.2019.109339.
[33] Maia MM. Techno-economic analysis of green ammonia production using offshore wind farms. M.Sc. Thesis. Iceland School of Energy at Reykjavík University; 2021.
[34] Di Lullo G, Giwa T, Okunlola A, Davis M, Mehedi T, Oni A, Kumar A. Large-scale long-distance land-based hydrogen transportation systems: a comparative techno-economic and greenhouse gas emission assessment. Int J Hydrogen Energy 2022;47(83):35293–319. https://doi.org/10.1016/j.ijhydene.2022.08.131. https://www.sciencedirect.com/science/article/pii/S036031992203659X.
[35] Raab M, Körner R, Dietrich R-U. Techno-economic assessment of renewable hydrogen production and the influence of grid participation. Int J Hydrogen Energy 2022;47(63):26798–811. https://doi.org/10.1016/j.ijhydene.2022.06.038. https://www.sciencedirect.com/science/article/pii/S0360319922025903.
[36] Smith C, Hill AK, Torrente-Murciano L. Current and future role of haber–bosch ammonia in a carbon-free energy landscape. Energy Environ Sci 2020;13(2):331–44.
[37] Bicer Y, Dincer I, Vezina G, Raso F. Impact assessment and environmental evaluation of various ammonia production processes. Environ Manag 2017;59(5):842–55. https://doi.org/10.1007/s00267-017-0831-6.
[38] Arora P, Sharma I, Hoadley A, Mahajani S, Ganesh A. Remote, small-scale, 'greener' routes of ammonia production. J Clean Prod 2018;199:177–92. https://doi.org/10.1016/j.jclepro.2018.06.130.
[39] Ghavam S, Vahdati M, Wilson IAG, Styring P. Sustainable ammonia production processes. Front Energy Res 2021;9. https://doi.org/10.3389/fenrg.2021.580808.
[40] Erdemir D, Dincer I. A perspective on the use of ammonia as a clean fuel: challenges and solutions. Int J Energy Res 2021;45(4):4827–34. https://doi.org/10.1002/er.6232.
[41] Technical University of Denmark (Dtu). Global wind atlas. 2022. accessed: https://globalwindatlas.info.
[42] Solargis s.r.o.. Global solar atlas. 2022. accessed, https://globalsolaratlas.info.
[43] Neyriz climate weather averages. 2022. https://www.worldweatheronline.com/neyriz-weather-averages/fars/ir.aspx.
[44] Ghazinoory S, Khosravi M, Nasri S. A systems-based approach to analyze environmental issues: problem-oriented innovation system for water scarcity problem in Iran. J Environ Dev 2021;30(3):291–316. https://doi.org/10.1177/10704965211019084.
[45] Madani K, AghaKouchak A, Mirchi A. Iran's socio-economic drought: challenges of a water-bankrupt nation. Iran Stud 2016;49(6):997–1016. https://doi.org/10.1080/00210862.2016.1259286.
[46] Lo J. Drought and water mismanagement spark deadly protests in Iran. 28.07.2021. https://www.climatechangenews.com/2021/07/28/drought-and-water-mismanagement-spark-deadly-protests-in-iran/.
[47] Cavaliere PD, Perrone A, Silvello A. Water electrolysis for the production of hydrogen to be employed in the ironmaking and steelmaking industry. Metals 2021;11(11):1816. https://doi.org/10.3390/met11111816.
[48] NEL. NEL hydrogen electrolyzers datasheet. 2021. https://nelhydrogen.com/water-electrolysers-hydrogen-generators/.
[49] Thyssenkrupp. Large-scale water electrolysis for green hydrogen production datasheet. 2020. https://thyssenkrupp-nucera.com/green-hydrogen-solutions/.
[50] Curto D, Franzitta V, Guercio A. A review of the water desalination technologies. Appl Sci 2021;11(2):670. https://doi.org/10.3390/app11020670.
[51] Morgan ER, Manwell JF, McGowan JG. Sustainable ammonia production from u.s. offshore wind farms: a techno-economic review. ACS Sustainable Chem Eng 2017;5(11):9554–67. https://doi.org/10.1021/acssuschemeng.7b02070.
[52] Chen Q, Burhan M, Shahzad MW, Ybyraiymkul D, Akhtar FH, Li Y, Ng KC. A zero liquid discharge system integrating multi-effect distillation and evaporative crystallization for desalination brine treatment,. Desalination 2021;502:114928. https://doi.org/10.1016/j.desal.2020.114928.
[53] Bossel U, Eliasson B, Taylor G. The future of the hydrogen economy: Bright or bleak. Cogener Distrib Gener J 2003;18(3):29–70. https://doi.org/10.1080/15453660309509023.
[54] Morgan Eric R. Techno-economic feasibility study of ammonia plants powered by offshore wind. Ph.D. Thesis, Department of Mechanical and Industrial Engineering. University of Massachusetts Amherst; 2013. https://doi.org/10.7275/11KT-3F59.
[55] Shashi Menon E. Chapter eight - power required to transport. In: Shashi Menon E, editor. Transmission pipeline calculations and simulations manual. Boston: Gulf Professional Publishing; 2015. p. 317–27. https://doi.org/10.1016/B978-1-85617-830-3.00008-0.

[56] Cheema II, Krewer U. Operating envelope of haber–bosch process design for power-to-ammonia. RSC Adv 2018;8(61):34926–36. https://doi.org/10.1039/C8RA06821F.
[57] Moran MJ, Shapiro HN, Boettner DD, Bailey MB. Fundamentals of engineering thermodynamics. 8th ed. Hoboken, NJ: Wiley; 2014.
[58] Araújo A, Skogestad S. Control structure design for the ammonia synthesis process. Comput Chem Eng 2008;32(12):2920–32. https://doi.org/10.1016/j.compchemeng.2008.03.001.
[59] Appl M. Ammonia: principles and industrial practice. Weinheim and New York: Wiley; 1999. https://doi.org/10.1002/9783527613885. https://onlinelibrary.wiley.com/doi/book/10.1002/9783527613885.
[60] Morgan E, Manwell J, McGowan J. Wind-powered ammonia fuel production for remote islands: a case study. Renew Energy 2014;72:51–61. https://doi.org/10.1016/j.renene.2014.06.034.
[61] ASMEB31.4. Pipeline transportation systems for liquid hydrocarbons and other liquids: ASME code for pressure piping. 2006. B31, https://www.asme.org/codes-standards/find-codes-standards/b31-4-pipeline-transportation-systems-liquids-slurries/2006/drm-enabled-pdf.
[62] A. B31.12. Hydrogen piping and pipelines: ASME code for pressure piping. 2011. B31, https://www.asme.org/codes-standards/find-codes-standards/b31-12-hydrogen-piping-pipelines/2011/drm-enabled-pdf.
[63] Shashi Menon E. Chapter four - pipeline stress design. In: Shashi Menon E, editor. Transmission pipeline calculations and simulations manual. Boston: Gulf Professional Publishing; 2015. p. 83–148. https://doi.org/10.1016/B978-1-85617-830-3.00004-3.
[64] González Díez N, van der Meer S, Bonetto J, Herwijn A. Technical assessment of Hydrogen transport, compression, processing offshore. 2020. https://north-sea-energy.eu/static/7ffd23ec69b9d82a7a982b828be04c50/FINAL-NSE3-D3.1-Final-report-technical-assessment-of-Hydrogen-transport-compression-processing-offshore.pdf.
[65] Dechant D, Bambei JH. Steel pipe – a guide for design and installation. Denver CO: American Water Works Association; 2017. 5th Edition, Vol. M11 of Manual of water supply practices, https://engage.awwa.org/PersonifyEbusiness/Store/Product-Details/productId/62572078.
[66] Menon ES. Chapter 8-pipeline hydraulic analysis. In: Pipeline planning and construction Field manual. Boston: Gulf Professional Publishing; 2011. p. 123–75. https://doi.org/10.1016/B978-0-12-383867-4.00008-6.
[67] ASME B36.10M. Welded and seamless wrought steel pipe. 2018. https://www.asme.org/codes-standards/find-codes-standards/b36-10m-welded-seamless-wrought-steel-pipe/2018/drm-enabled-pdf.
[68] Shashi Menon E. Chapter five - fluid flow in pipes. In: Shashi Menon E, editor. Transmission pipeline calculations and simulations manual. Boston: Gulf Professional Publishing; 2015. p. 149–234. https://doi.org/10.1016/B978-1-85617-830-3.00005-5.
[69] Shashi Menon E. Chapter six - pressure required to transport. In: Shashi Menon E, editor. Transmission pipeline calculations and simulations manual. Boston: Gulf Professional Publishing; 2015. p. 235–72. https://doi.org/10.1016/B978-1-85617-830-3.00006-7.
[70] Roth A, Brückmann R, Jimeno M, Đukan M, Kitzing L, Breitschopf B, Alexander-Haw A, Lucia A, Blanco Amazo. Renewable energy financing conditions in Europe. European Commission Horizon 2021;2020. http://aures2project.eu/2021/06/29/renewable-energy-financing-conditions-in-europe-survey-and-impact-analysis/.
[71] Rezaei M, Khalilpour KR, Jahangiri M. Multi-criteria location identification for wind/solar based hydrogen generation: the case of capital cities of a developing country. Int J Hydrogen Energy 2020;45(58):33151–68. https://doi.org/10.1016/j.ijhydene.2020.09.138.
[72] Aguilar LA, Mayer J, Ghafouri MH, Khosroshahi N, Grundner C, Vasaf E, Haid S, Mahdavi S, Mahmoudi A, Jafarkazemi F. Enabling PV Iran: the emerging PV market in Iran, German Solar Association – BSW-Solar/Bundesverband Solarwirtschaft e.V., Berlin. 2015. https://www.solarwirtschaft.de/datawall/uploads/2020/04/AA_Report_BSW_Iran-1.pdf.
[73] Cole W, Frazier AW, Augustine C. Cost projections for utility-scale battery storage: 2021 update, National Renewable Energy Laboratory (NREL). 2021. https://doi.org/10.2172/1786976.
[74] L. Bertuccioli, A. Chan, D. Hart, F. Lehner, B. Madden, E. Standen, (2014). URL https://www.e4tech.com/resources/107-development-of-water-electrolysis-in-the-european-union.php?filter=year%3A2014.
[75] Brynolf S, Taljegard M, Grahn M, Hansson J. Electrofuels for the transport sector: a review of production costs,. Renew Sustain Energy Rev 2018;81:1887–905. https://doi.org/10.1016/j.rser.2017.05.288.
[76] Elberry AM, Thakur J, Santasalo-Aarnio A, Larmi M. Large-scale compressed hydrogen storage as part of renewable electricity storage systems. Int J Hydrogen Energy 2021;46(29):15671–90. https://doi.org/10.1016/j.ijhydene.2021.02.080.
[77] Parks G, Boyd R, Cornish J, Remick R. Hydrogen station compression, storage, and dispensing: technical status and costs, Golden, CO. 2014. https://www.nrel.gov/docs/fy14osti/58564.pdf.
[78] Jepma C, Kok G-J, Renz M, van Schot M, Wouters K. Towards sustainable energy production on the North Sea - green hydrogen production and CO2 storage: onshore or offshore?. 2018.
[79] Desalination Committee (white paper), Overview of desalination plant intake alternatives. 2011. https://watereuse.org/wp-content/uploads/2015/10/Intake_White_Paper.pdf.
[80] Fúnez Guerra C, Reyes-Bozo L, Vyhmeister E, Jaén Caparrós M, Salazar JL, Clemente-Jul C. Technical-economic analysis for a green ammonia production plant in Chile and its subsequent transport to Japan. Renew Energy 2020;157:404–14. https://doi.org/10.1016/j.renene.2020.05.041.
[81] Buttler A, Spliethoff H. Current status of water electrolysis for energy storage, grid balancing and sector coupling via power-to-gas and power-to-liquids: a review,. Renew Sustain Energy Rev 2018;82:2440–54. https://doi.org/10.1016/j.rser.2017.09.003.
[82] Rinker GT. Development of a mechanical vapor-compression distiller incorporating concentrated solar power, M.Sc. Thesis, Mechanical engineering, West Virginia University. 2014.
[83] Seider WD. Product and process design principles: synthesis, analysis, and evaluation. 3rd ed. Hoboken NJ: Wiley; 2009.
[84] NIOC. Cost estimation guide for projects (feasibility phase): pump and compressor stations, Iran. 2015. https://cpm.nioc.ir/Project_Cost_Estimation/Reports/Chapter4-960412.pdf.
[85] HOMER Pro Simulation Platform. 2022., Version 3.15. https://www.homerenergy.com/products/pro/docs/latest/index.html.
[86] Moshiri S, Lechtenböhmer S. Sustainable energy strategy for Iran, Wuppertal Institute for climate. Environment and Energy, Wuppertal, Germany 2015. https://epub.wupperinst.org/frontdoor/deliver/index/docId/6175/file/WS51.pdf.

[87] Temiz M, Javani N. Design and analysis of a combined floating photovoltaic system for electricity and hydrogen production. Int J Hydrogen Energy 2020;45(5):3457–69. https://doi.org/10.1016/j.ijhydene.2018.12.226.
[88] Kalinci Y, Hepbasli A, Dincer I. Techno-economic analysis of a stand-alone hybrid renewable energy system with hydrogen production and storage options. Int J Hydrogen Energy 2015;40(24):7652–64. https://doi.org/10.1016/j.ijhydene.2014.10.147.
[89] Ardelean M, Minnebo P. HVDC submarine power cables in the world : state-of-the-art knowledge, European Union, Joint Research Centre Technical Report. 2015. https://doi.org/10.2790/023689.
[90] Ammonia price trend and forecast: market overview. 2022. https://www.chemanalyst.com/Pricing-data/ammonia-37.
[91] Demirhan CD, Tso WW, Powell JB, Pistikopoulos EN. Sustainable ammonia production through process synthesis and global optimization. AIChE J 2019;65(7):e16498. https://doi.org/10.1002/aic.16498.
[92] Tsatsaronis G. Challenges associated with the use of hydrogen for decarbonization, in: international symposium and workshop, sustainable solutions at times of transition (SuST). Nisyros, Greece July 14-17, 2022.
[93] Tavanir, Iran. 2016. https://rise.esmap.org/data/files/library/iran,-islamic-rep./Cross%20Cutting/CC.11..pdf.
[94] Tiseo I. Carbon intensity of the power sector in Germany from 2000 to 2021: (in grams of CO_2 per kilowatt-hour. Stat 2022. https://www.statista.com/statistics/1290224/carbon-intensity-power-sector-germany/.